Part 1: Screening of selected molecules for their effect on the secondary structure of amyloid beta.

Part 2: Composition and biological activity of traditional and commercial kava extracts.

Cynthia S. Côté

A thesis submitted to McGill University in partial fulfillment of the requirements of the degree of Master of Science.

Department of Chemistry
McGill University, Montréal
April, 2006

Your file Votre référence
ISBN: 978-0-494-24646-7
Our file Notre référence
ISBN: 978-0-494-24646-7

ABSTRACT

The aim of the first project was to evaluate the ability of selected molecules to affect the secondary structure of $A\beta_{(1-42)}$. Such activity is desirable as it may provide new tools to study the role of the $A\beta_{(1-42)}$ conformers in Alzheimer disease. Although this study did not identify molecules able to modulate the conformation of $A\beta_{(1-42)}$, the reported studies have set the fundamental techniques for this project.

The goal of the second project was to compare the kavalactone content and the inhibition of human P450 enzymes for commercial and traditional kava extracts. We report that amounts and ratios of kavalactones are similar for solvents that mimic commercial extracts but different from aqueous extract (traditional extract). All extracts tested show similar inhibition of the P450 enzymes suggesting that kava extracts, commercial or traditional, may lead to herb-drug interactions. These results also suggest that because of their higher concentration of kavalactones, commercial kava extracts are more likely to cause adverse drug reactions via inhibition of drug metabolism.

RESUME

L'objectif du premier projet était d'évaluer l'effet de certaines molécules sur la structure secondaire de l'amyloid beta (1-42). Une telle activité est souhaitable puisqu'elle pourrait procurer des outils importants pour étudier le rôle de la structure secondaire de l'$A\beta_{1-42}$ dans la maladie d'Alzheimer. Même si cette étude n'a pas permis d'identifier des molécules actives, elle nous a permis d'optimiser un ensemble de techniques fondamentales pour la suite de ce projet.

Le but du deuxième projet était de comparer la composition et l'inhibition des enzymes P450 humaines de différents extraits de kava simulant les extraits traditionnel ou commerciaux. Nous avons déterminé que la quantité et les ratios de kavalactones sont similaires pour les extraits qui simulent les extraits commerciaux, mais varient comparé à l'extrait traditionnel aqueux. En conclusion, tous les extraits testés montrent une inhibition similaire de l'activité des P450s, suggérant que les deux types d'extraits, traditionnel et commercial, peuvent conduire à des interactions herbe-médicaments.

REMERCIEMENTS

Premièrement, j'aimerais remercier ma directrice de recherche la docteure Karine Auclair pour ses précieux conseils. Son enthousiasme et l'originalité de ses projets de recherche témoignent de sa passion pour la chimie bio-organique et les domaines qui s'y rattachent. Deuxièmement, j'aimerais remercier monsieur Nadim Saade pour son assistance dans l'obtention et l'analyse de spectres de masse et pour sa promptitude lors de situations impérieuses. Également, j'aimerais remercier le docteur Paul Xia pour son assistance dans l'obtention de spectres de résonances magnétiques nucléaires.

Je tiens à exprimer ma reconnaissance à la Faculté des Études Graduées de l'Université McGill, au Département de Chimie de l'Université McGill ainsi qu'à l'Instituts de Recherche en Santé du Canada pour leurs assistances financières.

Je remercie mes collègues Christine Caputo, Amandine Chefson, John Cohen, Feng Gao, Cédric Gaudineau, Stephen Jackson, Christine Kor, Janice Lawandi, la docteure Samia Ait-Mohand, Xuxu Yan et Jin Zhao. De plus, je tiens à remercier les personnes suivantes : Nathalie Bousquet-Gagnon, Amandine Chefson, Feng Gao, Mylène Gravel, Tobie Généreux Vincent, Christine Kor, Janice Lawandi et la docteure Samia Ait-Mohand pour leurs encouragements et leurs amitiés.

J'aimerais exprimer mon affection ainsi que ma reconnaissance à ma famille Jean-Marc, Marguerite, Sarah, Olivia et Jean-Paul Bougie; Rita, Jean-François, Marc-André, David, Antoine-Derick, Carl-Olivier et Amélia-Ann Côté; Eve Deapen, Nathalie Vachon et Régine Santerre pour cette affection réciproque et pour avoir toujours cru en moi. Plus particulièrement, je remercie de tout mon cœur mes parents Richard et Diane Côté pour leur soutient tant affectif que financier.

Finalement, mon plus gros remerciement revient à Steve Bougie, mon conjoint. Il a toujours cru en moi et il m'a constamment encouragée. Ta bonne humeur contagieuse, ton implication dans tout mes projets autant personnels qu'académiques et par dessus tout ton amour m'ont aidé à terminer cette maîtrise.

Mille mercis à tous et chacun!

TABLE OF CONTENTS

ABBREVIATIONS

Å	.....	armstrong
Aβ		Amyloid-beta peptide
AHMC	.....	3-[2-*N*,*N*-diethyl-*N*-methylamino)ethyl]-7-hydroxy-4-methylcoumarin
Ala	.....	alanine
AMMC	.....	3-[2-(*N*,*N*-diethyl-*N*-methylamino)ethyl]-7-methoxy-4-methylcoumarin
APCI	.....	atmospheric pressure chemical ionization
APP	.....	amyloid beta precursor protein
Asp	.....	aspartic acid
$A\beta_{(1-42)}$	.....	amyloid beta (1-42) peptide
BFC	.....	7-benzyloxy-4-trifluoromethylcoumarin
Boc	.....	*N*-(*tert*-butoxycarbonyl)
Calcd	.....	calculated
CD	.....	circular dichroism
CPR	.....	cytochrome P450 reductase
CYP	.....	cytochrome P450 enzyme
DCM	.....	dimethyl chloride
deg	.....	degree
DHK	.....	dihydrokavain
DHM	.....	dihydromethysticin
DIPEA	.....	*N*,*N*-diisopropylethylamine
DMF	.....	*N*,*N*-dimethylformamide

dmol ..... decimole

DMY ..... demethoxyyangonin

ER ..... ethoxyresorufin

Fmoc ..... *N*-(9-fluorenylmethoxycarbonyl)

FTIR ..... fourrier transform infrared spectroscopy

g ..... gram

GABA ..... γ-aminobutyric acid

HATU ..... *O*-(7-azabenzotriazol-1-yl)-*N,N,N',N'*-tetramethyluronium hexafluorophosphate

HFC 7-hydroxy-4-trifluoromethylcoumarin

HFIP 1,1,1,3,3,3-Hexafluoroisopropanol

HPLC ..... high performance liquid chromatography

Hz ..... hertz

IC_{50} ..... inhibitor concentration required to get 50% inhibition of an enzyme activity

K ..... kavain

KL ..... kavalactones

LC-MS ..... liquid chromatography mass spectroscopy

LRMS ..... low resolution mass spectroscopy

Lys ..... lysine

M ..... methysticin

MFC 7-methoxy-4-trifluorocoumarin

M ..... molar

mg ..... miligram

MHz ..... megahertz

min ..... minute

ml ..... mililiter

mol ..... mole

MRW ..... mean residue weight

NADP ..... nicotinamide adenine dinucleotide phosphate, oxidized form

NADPH ..... nicotinamide adenine dinucleotide phosphate, reduced form

nm ..... nanometer

NMR ..... nuclear magnetic resonnance

P450 ..... cytochrome P450 enzyme

RH ..... typical substrate of P450 enzymes

ROH ..... product of the action of P450 enzymes on RH

sec .....second

Ret. .....retention

TFA ..... trifluoroacetic acid

TFE .....trifluoroethanol

UV ..... ultraviolet

v/v ..... volume/volume

w/v ..... weight/volume

Y ..... yangonin

α ..... alpha

β	..... beta
γ	..... gamma
δ	.....chemical shift in ppm
μ	.....micron
λ	..... wavelength
λem	..... emission wavelength
λex	..... excitation wavelength
μl	..... microliter

LIST OF SCHEMES

LIST OF FIGURES

LIST OF TABLES

PREAMBLE TO THESIS

This thesis contains two distinct subjects which will be treated separately in chapters one and two. In chapter one, we present the preliminary results obtained for the study of specific molecules and their effect on the secondary structure of amyloid beta (1-42) peptide. In chapter two, we present our results on the composition and biological activity of traditional and commercial kava extracts.

CONTRIBUTIONS OF THE CO-AUTHORS

The majority of small molecules presented in chapter one were designed and synthesized by Dr Samia Ait-Mohand and two were prepared by Cynthia S. Côté. All HPLC and circular dichroism analysis were performed by Cynthia S. Côté. The article presented in chapter two is co-authored by Cynthia S. Côté, Christine Kor, John Cohen and Dr. Karine Auclair. Cynthia S. Côté achieved most of the work presented in this article. Christine Kor contributed to the studies related to the inhibition of CYP2C9 and CYP2C19. John Cohen participated in the preliminary optimization of CYP3A4 inhibition assay. All authors have read and approved the final manuscript. Copyright of the article is annexed at the end of the thesis.

Chapter 1: Screening of selected molecules for their effect on the secondary structure of amyloid beta

1.1 LITERATURE REVIEW

1.1.1 Peptide and protein structure

Proteins and peptides adopt three-dimensional structures that can be described at four different levels. The primary structure of a protein or a peptide is defined by its amino acid sequence. The secondary structure describes the local three-dimensional backbone arrangement of a short contiguous peptide segment (3-30 residues). The tertiary structure is determined by the three-dimensional interactions (intramolecular) between the different secondary structure elements. Finally, the quaternary structure is defined by the number, the type and the spatial arrangement of the polypeptide units forming an oligomeric protein. Characteristics of secondary structures will be described in more details, because they are the subject of this thesis[1].

1.1.1.1 Secondary structure

The backbone of a peptide consists of a repetition of three types of bonds: the bond between the α-carbon and the carbonyl carbon, the bond between the carbonyl carbon and the α-nitrogen (termed peptide bond), and the bond between the α-nitrogen and the α-carbon. The possible conformations adopted by the peptide backbone can be characterized by the torsion angles between these bonds, termed psi (ψ), phi (φ) and omega (ω) respectively. The resonance between the carbonyl and the nitrogen atom confers a partial double bond character to the peptide bond, thus limiting its rotation. The peptide bond is considered planar and therefore its ω value is 120° (Figure 1A). As a result, the secondary structure is characterized by a combination of ψ and φ. The propensity of an amino acid to adopt a given secondary structure is highly dependent on the environment but also on the

nature of its side chain. The propensity of each amino acid to form helical, β-sheet and random coil secondary structures was determined by Chou and Fasman and is summarized in Table 1[2]. Propensities were calculated to determine the likelihood of a given amino acid to adopt one of different structures. Higher numbers increase the likelihood that a peptide portion will adopt a specific structure. For a given secondary structure, propensities above 1 for six consecutive residues suggest that this portion of the peptide will likely fold according to this structure.

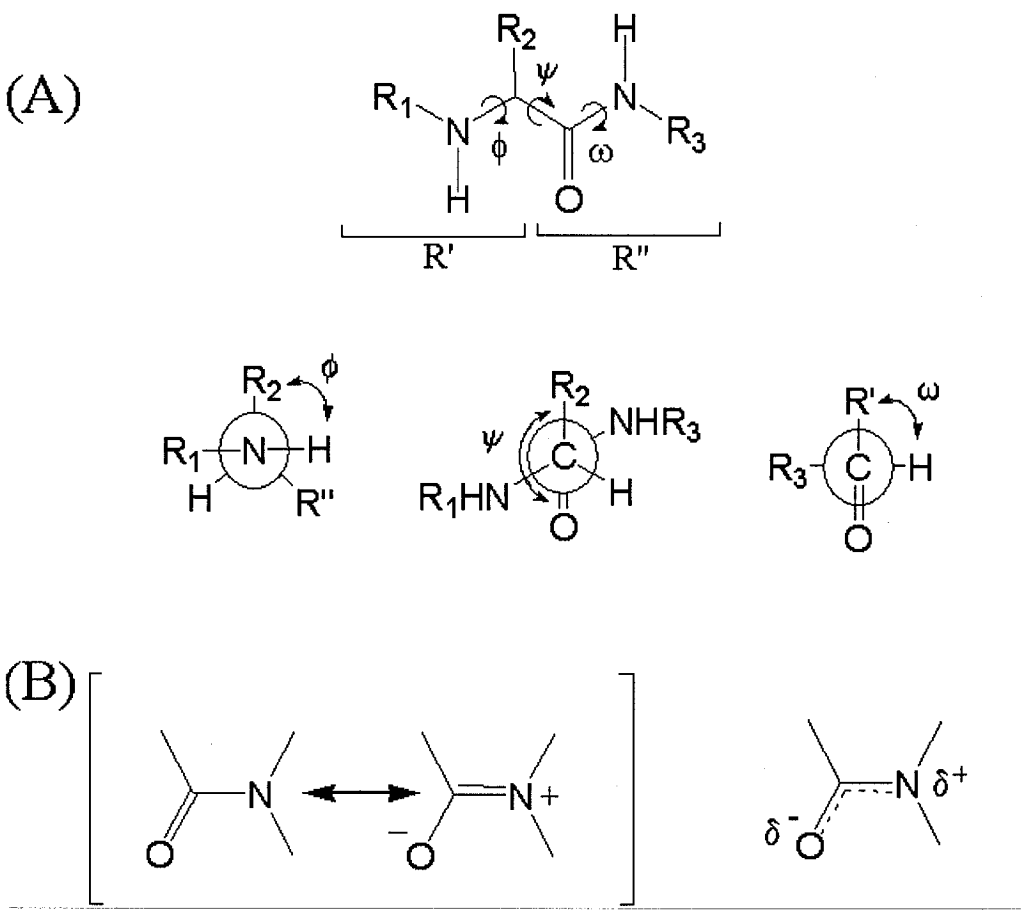

Figure 1 - (A) Torsion angles phi (φ), psi (ψ) and omega (ω) for the peptide backbone. (B) Peptide bond resonance structure conferring a partial double bond character.

Table 1 - Secondary structure propensity for natural amino acids[2].

Amino acid	Helix	β-Sheet	Random Coil	Amino acid	Helix	β-Sheet	Random Coil
Alanine	1.42	0.83	0.75	Methionine	1.45	1.05	0.5
Cysteine	0.7	1.19	1.11	Asparagine	0.67	0.89	1.44
Aspartic acid	1.01	0.54	1.45	Proline	0.57	0.55	1.88
Glutamic acid	1.51	0.37	1.12	Glutamine	1.11	1.1	0.79
Phenylalanine	1.13	1.38	0.49	Arginine	0.98	0.93	1.09
Glycine	0.57	0.75	1.68	Serine	0.77	0.75	1.48
Histidine	1	0.87	1.13	Threonine	0.83	1.19	0.98
Isoleucine	1.08	1.6	0.32	Valine	1.06	1.7	0.24
Lysine	1.16	0.74	1.1	Tryptophan	1.08	1.37	0.45
Leucine	1.21	1.3	0.49	Tyrosine	0.69	1.47	0.84

1.1.1.1.1 Peptide helices

In helices the peptide backbone is twisted and the amino acid side chains point outside the helix (Figure 2). This structure is stabilized by hydrogen bonds between the oxygen of an α-carbonyl and the hydrogen atom on the α-nitrogen three or four residues away (Figure 2). The different types of helices; α-helix, 3_{10}-helix and π-helix, are defined by the number of residues per turn (n), the distance between consecutive turns, termed pitch (h), torsion angle ψ and φ (Table 2) and the number of atom contained in the ring formed by the intramolecular hydrogen bond (r) (Figure 2). The α-helix is the common important helix type because of its higher relative stability[3].

Five types of interactions may affect the stability of helices. The first one is the electrostatic interactions (attraction or repulsion) between side chains of two adjacent amino acids. The second one is the bulkiness of two successive amino acids side chains. The third type of interactions affecting stability is that between amino acid side chains spaced by three residues (i, i+4). The presence of proline residues, which can't form hydrogen bond to stabilize the helical structure also greatly affects helix stability. Finally, amino acid residues at the helix termini (C-ternimal and N-ternimal) cannot form stabilizing hydrogen bonds. To compensate, natural systems often provide hydrogen bonds via side chains of other residues from the protein. This form of capping is believed to stabilize the helices termini[4,5].

Table 2 - Helix types characteristics.

Helix name	Ψ (°)	Φ (°)	n (amino acids)	h (nm)	r (member)
A-Helix	-47	57	3.6	0.540	13
3_{10}	-30	-60	3	0.600	10
π-Helix	-70	-57	4.4	0.528	16
Polyproline I	+158	-83	-3.0	0.930	-
Polyproline II	+149	-78	3.3	0.560	-
Polyglycine II	+150	-80	3.0	0.900	-

Ψ = psi, Φ = phi, n = number of residues per turn, h = pitch and r = number of atoms in the intramolecular ring formed by a hydrogen bond

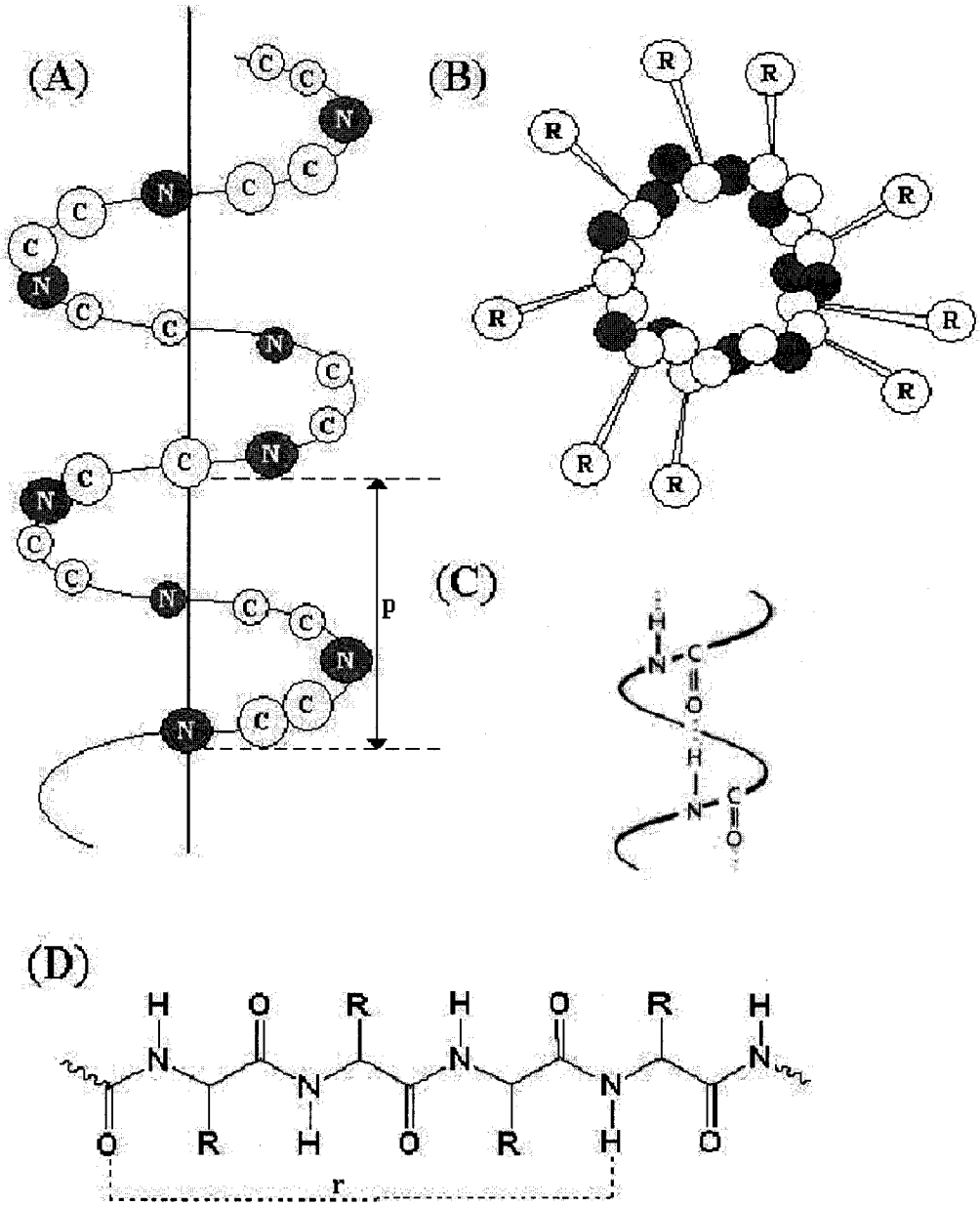

Figure 2 - (A) Representation of a peptide helix. (B) Longitudinal view of the α-helix structure showing the amino acid side chains (R) projecting outside of the helix. When Van der Waals radii inside the helix are taken into account, there is almost no free space inside the helix. (C) Hydrogen bonds involved in α-helices. (D) Linear view of the intramolecular ring hydrogen bonding important in α-helices.

1.1.1.1.2 β-Sheets

In β-sheet structures, the amino acids are organized in a pleated sheet, where the side chains of two consecutive residues point in opposite direction (Figure 3). In contrast to helices, the hydrogen bonds stabilizing the β-sheet structure do not occur inside a segment but between two adjacent segments. The segment constituting the β-sheet may be aligned parallel or antiparallel (Figure 3). In β-sheet, torsion angles ψ and φ often differ from the ideal values (-180° and 180°) to avoid distortion. This results on ψ/φ values of -139°/+135° and −119°/+113° for the antiparallel β-sheet and the parallel β-sheet respectively. As with helical structures, the major factor affecting β-sheet stability is the nature of the amino acid side chains. For example, glycine and proline (β-breaker), have a low propensity to form β-sheets and destabilizes them. The bulky five member ring of proline is not easily accommodated in β-sheets. In contrast, hydrophobic amino acids have a good propensity to form β-sheet structures[3].

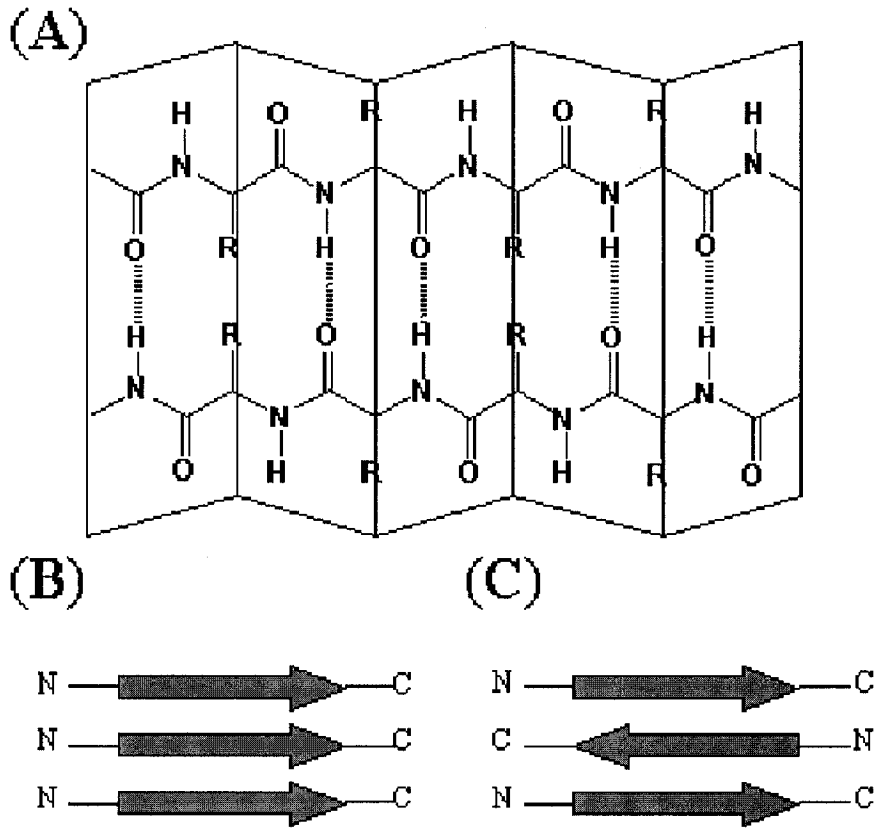

Figure 3– (A) Representation of β-pleated sheets and their hydrogen bonding pattern. (B) Parallel β-pleated sheets. (C) Antiparallel β-pleated sheets

1.1.1.1.3. Turns

Turns in polypeptides are characterized by an inversion of the peptide chain direction. The number of amino acids involved in a turn can be 3, 4, 5 or 6, corresponding to γ-, β-, α- and π-turns respectively. Turns are often stabilized by a hydrogen bond between the first and the last amino acid of the loop (Figure 4). Because of their geometry, proline and glycine amino acids have a high propensity to form turns[6].

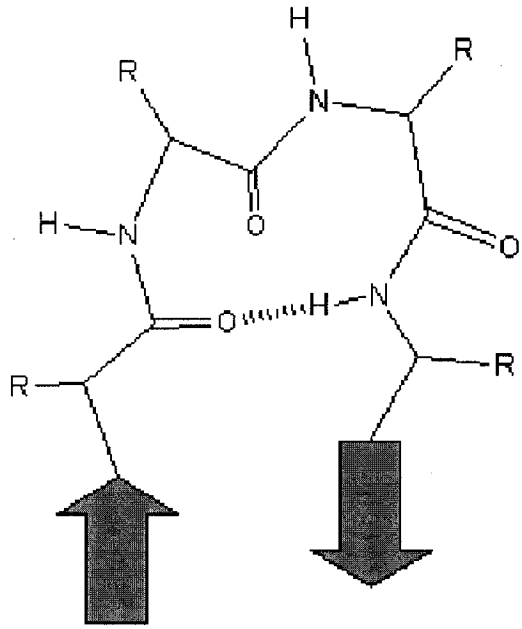

Figure 4– Representation of a β-turn stabilized by a hydrogen bond between the first and the last amino acids of the turn

1.1.1.2 Techniques to study protein and peptide secondary structures

Nowadays, X-ray crystallography and nuclear magnetic resonance (NMR) are the best techniques to obtain high resolution three-dimensional structures of proteins and peptides. Both techniques necessitate large amount of the protein or the peptide, are expensive and time consuming, and require a high level of expertise. For these reasons, they are often used to determine three-dimensional structure of a protein or a peptide, but rarely to investigate the effect of solvents, salts or ligands. Circular dichroism (CD) and Fourrier transform infrared spectroscopy (FTIR) are ideal for rapid evaluation of secondary structure under different conditions. CD analysis may be applied to determine the overall secondary or tertiary structure of a protein or a peptide at low concentration (0.01-0.1 mM). It is relatively inexpensive and requires low level of expertise. FTIR can also be

used but requires much higher protein or peptide concentrations (0.5-2 mM) and the use of expensive deuterated buffers.

1.1.3 Previous investigations of the factors that affect helical secondary structures.

Mutagenesis, rational design and the addition of ligands have been used to investigate the factors affecting protein or peptide structure. Numerous strategies have been developed to stabilize helical peptide structures. One strategy uses metals which coordinate to amino acids located at positions i and i+4 of the peptide (Figure 5)[7,8]. For example, two iminodiacetic acid lysines may be positioned at i and i+4 of a peptide and when a divalent metal such as Cu^{2+}, Co^{2+}, Ni^{2+}, Zn^{2+} or Cd^{2+} is added to the peptide solution, the acids coordinate to the metal thus stabilizing the α-helix structure. These interactions may be destroyed by the addition of a chelating agent such as EDTA. Another strategy to stabilize peptide helices is their cyclization through the linkage of two amino acids. A well positioned covalent bond between two residues may stabilize α-helices. Such a strategy was used by Shepherd *et al.* to design and synthesize a stable α-helical pentapeptide in which the side chains of Glu1 and Lys5 are cyclized via an amide bond. This pentapeptide was designed using molecular modeling to evaluate amino acids allowing cyclization of the side chains located at the termini of the pentapeptide and to select amino acids favouring the formation of hydrogen bonds through the backbone of the helical structure[9]. A third strategy to stabilize peptide helices involves helix capping. The α-helix structure is characterized by consecutive hydrogen-bonds between the carbonyl of the amino acid at position i and the amide of the residue at position i+4. This pattern is interrupted at the helix termini and results in destabilization. The term capping refers to the addition of extra hydrogen-bonds at the N- or the C-termini of a peptide. A number of capping molecules

covalently linked to one end of a peptide were successful at stabilizing helical structures[10,11,12,13]. Figure 5 illustrates capping of a helical peptide and its stabilization by the formation of an additional hydrogen bond. The results reported by Maeda *et al.* differ in the intermolecular nature of the interactions used to stabilize helical peptides. Side chains of a small ligand were selected in order to form stabilizing salt bridges and hydrophobic interactions with the side residue at the termini of an helical peptide[14].

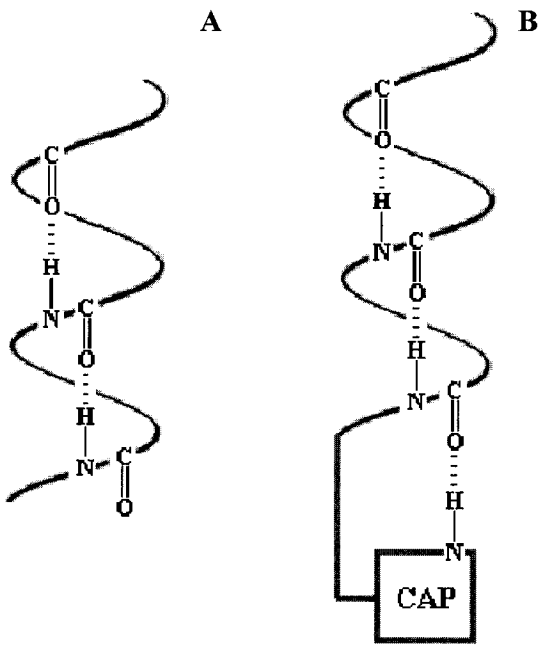

Figure 5– A: Illustrates the characteristic hydrogen bonding pattern of the helical structure and its interruption at the helix termini resulting in destabilization. B: Illustrates the stabilization of the helical structure by the formation of an additional hydrogen bond with a capping molecule.

Finally, fluorinated solvents such as 1,1,1,3,3,3-hexafluoroisopropanol and 2,2,2-trifuoroethanol are known to stabilize helical peptides[15]. Despite the widespread use of fluorinated solvents to stabilize helices, the mechanism of action remains debated. Molecular dynamics and NMR studies suggest that fluorinated solvents aggregate around

peptides and displace the water molecules implicated in hydrogen bonds within the amino acid backbone, therefore favoring intramolecular interactions such as those observed in helices[16,17]. Recent spectroscopic evidences suggest that desolvation fortifies the formation of intrahelical hydrogen bonds which stabilizes the helical structure[18]. The desolvation of peptides is also believed to increase helix stability by deordering water molecules and increasing their entropy[18].

1.1.2 The amyloid beta peptide (Aβ)

1.1.2.1 Formation of amyloid beta peptide (Aβ) and its relevance to Alzheimer disease

Amyloid diseases such as Alzheimer, Down syndrome, Parkinson, Huntington, type II diabetes, cystic fibrosis and prion diseases are characterized by protein misfolding events involving the conversion of generally soluble proteins into aggregates which eventually form amyloid fibrils. Once initiated, this phenomenon propagates until the aggregates or deposits induce organ failure and death. Although the proteins involved in these diseases are distinct, the resulting amyloids share several common features. Observation under the electronic microscope reveals fibrils of similar shape and size (average of 100 Å in diameter and 10 nm in length)[19,20]. They also show green birefringence upon staining with Congo red and affect the fluorescence of thioflavin-T[21]. The fibrils formed are stable species that resist degradation by proteases and their X-ray diffraction pattern corresponds to cross β-sheet-rich structures[19,20].

Misfolded amyloid beta peptides (Aβ) are the major component of the fibrils observed in Alzheimer disease. Aβ originates from the amyloid beta precursor protein (APP). APP is a type I transmembrane protein, encoded by the gene at the locus 21q21.3, for which a

function has only been vaguely defined. Two proteolytic cuts are required to generate Aβ peptide from APP (Figure 6). First, the protease β-secretase cleaves the extracellular fragment of APP to generate the N-terminal portion of Aβ. Then, the protease γ-secretase cleaves the APP within its transmembrane region to form Aβ peptides with a length varying from 39 to 43 amino acids[22]. An alternative proteolytic pathway implicates α- and β-secretases to produce the shorter peptides βAPPs α-fragments (15 or 16 residues), which are believed to be non-amyloidogenic[23]. $A\beta_{1-40}$ is the predominant product of APP under physiological conditions[24]; however, $A\beta_{1-42}$ is the most abundant in amyloid plaques found in the brain of Alzheimer's patients[25].

We chose to focus on amyloid beta peptides (Aβ) to investigate peptide conformational changes occurring during amyloid formation. This choice was based on the fact that Aβ is involved in Alzheimer disease, a preponderant form of amyloidosis and the fourth cause of death in North America, yet the most costly disease for our society[26].

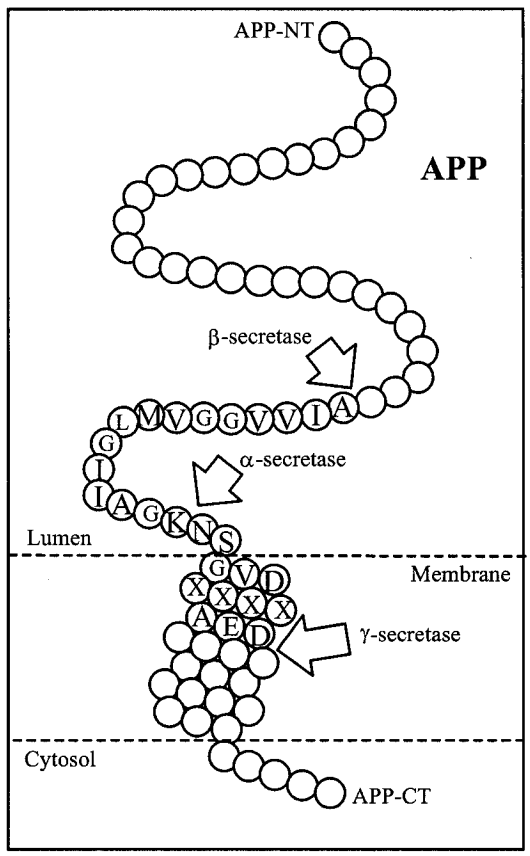

Figure 6 – Aβ formation from proteolytic cleavage of APP by β- and γ-secretase, or by α- and β-secretases yielding $A\beta_{1\text{-}40}$ and $A\beta_{1\text{-}42}$, or βAPPs (1-15) and (1-16) α-fragments respectively.

1.1.2.1. Amyloid beta fibril formation

The currently accepted Aβ fibril formation pathway is summarized in Figure 7. The first step consists of a conformational change from helical or random, to β-sheet. The β-sheets of Aβ next aggregate into soluble oligomers which grow to insoluble globular oligomers. Conversion of the globular oligomeric aggregates into protofibrils follows. Atomic force microscopy reveals that protofibrils present features of stacked peptides in a hairpin conformation perpendicular to the long axis of the protofibril[27,28]. Finally, protofibrils

assemble to form mature fibrils which present characteristic cross β-sheet-rich X-ray diffraction patterns[29] The fibrils range in size from 0.2 to 1.0 mm long and from 6 to 10 nm diameter[30,31]. Interestingly, the degree of dementia observed with Alzheimer's patients does not correlate well with the presence of senile plaques in the brain[32]. Some groups have suggested that soluble Aβ oligomers may be more toxic then the insoluble Aβ fibrils[33,34,35,36].

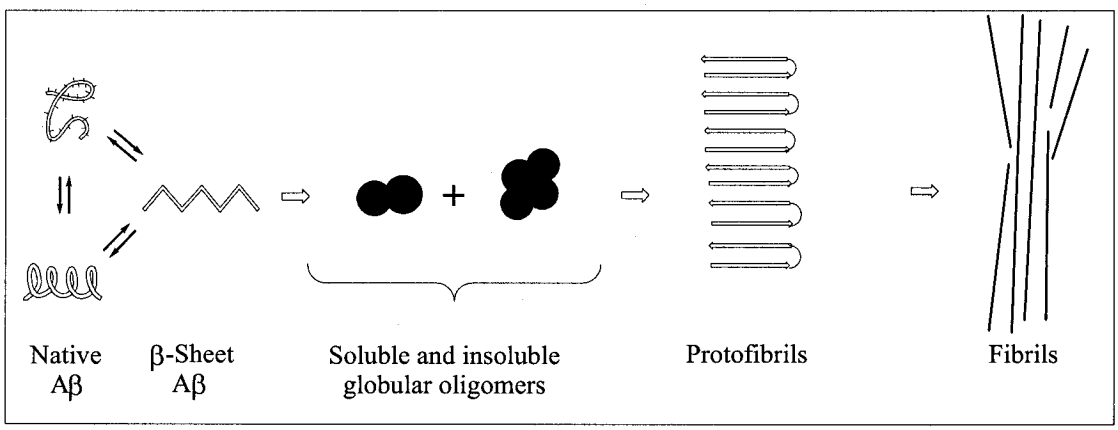

Figure 7 – Currently accepted steps involved in Aβ fibril formation: 1) Conformational change of Aβ to β-sheets; 2) Formation of soluble and insoluble globular oligomers; 3) Oligomers assembly into protofibrils; and 4) Fibril elongation via the linear combination of protofibrils.

One approach used by some pharmaceutical groups towards new treatments for Alzheimer disease is to directly inhibit oligomer formation of Aβ. This has been attempted using three different strategies. The first strategy uses metal chelators specific for metals known to stimulate Aβ aggregation (e.g. Fe^{3+} and Zn^{2+})[37,38]. The second approach is based on immunization. Antibodies against Aβ were reported to reverse fibril formation and inhibit Aβ toxicity in cells and rodents[39]. Unfortunately, a recent clinical study had to be stopped because of a high incidence of encephalitis[40]. Passive immunization is now showing encouraging results[41,42]. The last strategy consists of creating small molecules, which bind

to β-sheet Aβ with the aim of preventing their aggregation. Many of these molecules are peptides that contain amino acids which do not easily incorporate into β-pleated sheet structures (ex. proline and α-aminoisobutyric acid)[43,44,45,46,47,48]. Finally, non-peptidic molecules have also been reported to prevent Aβ aggregation[49,50,51,52].

1.1.3 Goal

As an alternative strategy, we hypothesized that Aβ aggregation could be inhibited by shifting the conformational equilibrium to favor the helical conformation of Aβ. We propose to design molecules that stabilize helical Aβ by binding to side chains of amino acids projecting on the same side of the helix, i.e. located at positions i and i+4 of the peptide (Figure 8).

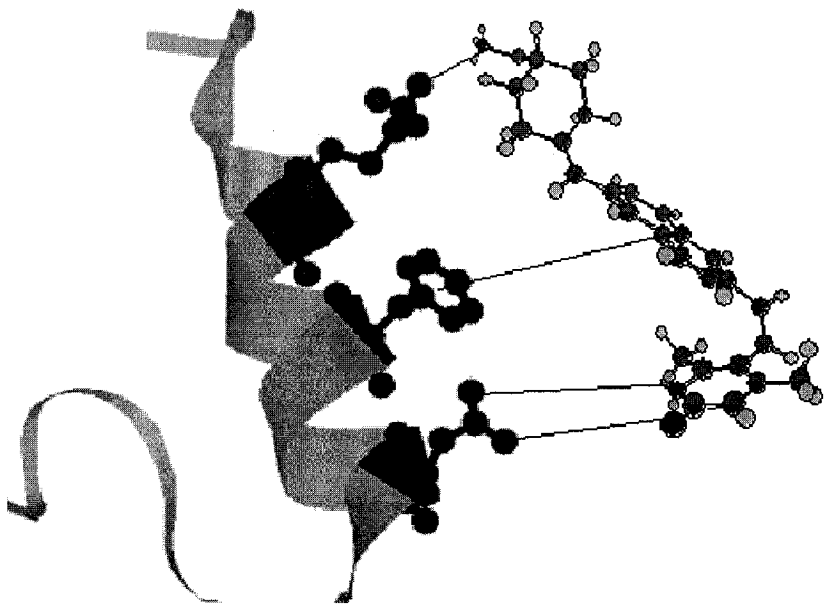

Figure 8 – Example of a ligand potentially stabilizing helical structure by ionic and hydrophobic interactions with amino acid side chains located at i, i+4 and i+8.

The target molecules were designed using recently published α-helical structures of $A\beta_{1-42}$ to calculate optimal parameters (distance, angles, etc...) for ionic and/or hydrophobic interactions with small molecules[53]. The length between each functional groups composing a target molecule was based on the distance between the targeted amino acid side chains i, i+4 and i+8. For example, the Lys^{16}, Phe^{19} and Asp^{23} residues selected on Aβ (Figure 8) were expected to interact with an acidic, an aromatic and a basic functional groups located on the designed small molecule. Molecules favoring helical Aβ represent new tools to study the factors affecting the conformation of Aβ and the role of helical Aβ in Alzheimer disease. Moreover, such ligands may offer a new alternative for the treatment of the disease.

1.2 INTRODUCTION

The misfolding of proteins into amyloid fibrils is characterizing diseases, such as Alzheimer, Parkinson and Prion diseases[19,20]. These fibrils form protease-resistant deposits which lead to cell and organ dysfunction and ultimately to death. Discordant helices contain amino acid sequence that would predict a β-pleated sheet structure[54,55]. Interestingly, the presence of discordant helices in protein structure have been correlated to their ability to generate amyloid. In Alzheimer disease, fibrillar deposits, termed senile plaques, are essentially composed of amyloid beta peptides (Aβ) of a length between 39 and 43 amino acid residues.

The currently accepted pathway for formation of Aβ fibrils is initiated by a conformational change of Aβ from helical or random coil to β-pleated sheets (Figure 9). The misfolded peptides collapse into soluble oligomers which assemble into larger insoluble oligomers. The latter are the building blocks leading to the formation of protofribrils[27]. Finally, protofibrils assemble to form insoluble fibrils[28-29].

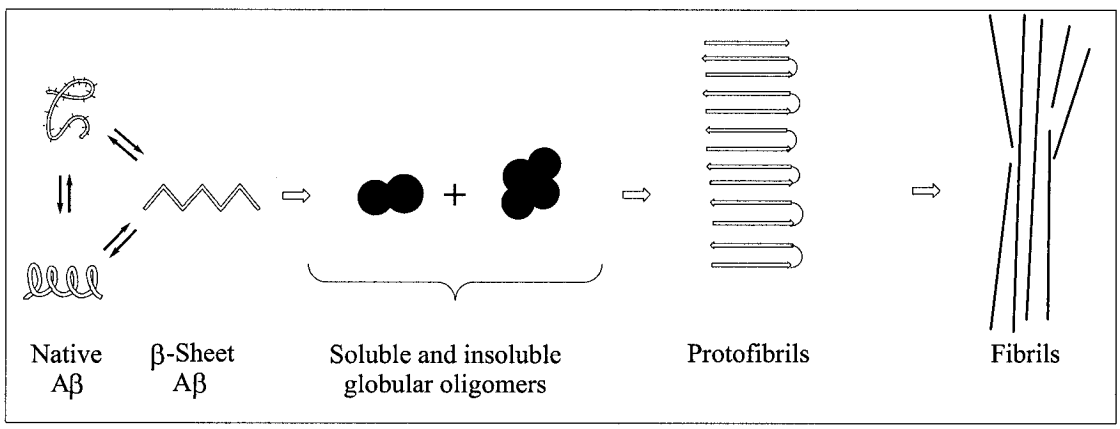

Figure 9 - Currently accepted steps involved in Aβ fibril formation: 1) Aβ changes conformation to β-strand structures that stack into β-sheets; 2) Soluble and insoluble

globular oligomers forms; 3) Oligomers assemble into protofibrils; and 4) Fibril elongation via the addition of protofibril subunits.

Some pharmaceutical groups focusing on Alzheimer disease attempt to inhibit Aβ oligomerization. To this end three different strategies had been used. The first strategy uses specific metal chelators[37-38] which chelate metals known to stimulate Aβ aggregation such as Fe^{3+} and Zn^{2+}. The second approach to control oligomerization of Aβ is based on immunization[39-42] and the last strategy uses small molecules, which bind to β-sheet Aβ and prevent their aggregation.

As an alternative strategy, we hypothesized that Aβ aggregation could be inhibited by favouring the helical conformation of Aβ. We propose to design molecules that stabilize helical Aβ by side-chain interactions with Aβ amino acids located on the same side of the helix, i.e. located at positions i and i+4 of the peptide. Those molecules represent new tools to study the effect of the conformation of Aβ on Alzheimer disease and may offer a new alternative for the treatment of the disease.

Stabilization of helical peptides was attempted using different strategies. Metals have been used to coordinate amino acids located at positions i and i+4 of a peptide[7,8]. The cyclization of amino acids positioned at i and i+4 of a peptide in some cases stabilized α-helices[9]. A third strategy to stabilize helices involves helix capping. The α-helix structure backbone is stabilized by an internal network of hydrogen-bonds between the carbonyl oxygens and amide nitrogens of residues at the positions i, i+4. This pattern is interrupted at the helix termini and results in destabilization. The term capping refers to the addition

of extra hydrogen-bonds at the N- or the C-terminus of a peptide. A number of capping molecules covalently linked to one end of a peptide were successful at stabilizing helical structures.[10-14] Finally, fluorinated solvents such as 1,1,1,3,3,3-hexafluoroisopropanol and 2,2,2-trifuoroethanol are also known to stabilize helical peptides via hydrophobic interactions that may keep water molecules away from the helix[15].

Herein we report the effect of 13 ligands designed to stabilize helical Aβ. CD spectroscopic studies did not reveal any significant effect of these molecules on the conformation of Aβ. These investigations have however allowed the development of methodologies to handle, purify, and evaluate the conformation of Aβ.

1.3 MATERIAL AND METHODS

1.3.1 Materials

Amyloid beta $_{(1\text{-}42)}$ (DAEFRHDSGYEVHHQKLVFFAEDVGSNKGAIIGLMVGGVVIA) was purchased from Service de Synthèse de Peptide de L'Est du Québec (Québec, QC, Canada) or from American Peptide Company (Sunnyvale, CA, USA). Amino acids and *O*-(7-azabenzotriazol-1-yl)-*N,N,N',N'*-tetramethyluronium hexafluorophosphate (HATU) were purchased from GL Biochem (Shanghai, China). HPLC grade acetonitrile and NH_4OH were purchased from Fischer Scientific (Ottawa, ON, Canada). Molecules **1-9** were synthesized in our laboratories by Dr. Samia Ait-Mohand. Their synthesis will be described elsewhere. All other chemicals were purchased from Sigma-Aldrich (St. Louis, MO, USA).

1.3.2 Instrumentation

CD spectra were obtained using a Jasco spectropolarimeter model J-810 equipped with a Pelletier thermostat model PTC-424s (Jasco Inc., Tokyo, Japan). The samples were examined using Spectrocil® 1-mm cuvettes (Starna Cells Inc., Atascadero, CA).

HPLC purifications were performed on an Agilent 1100 modular system equipped with an autosampler, a quaternary pump system, a photodiode array detector, a thermostatted column compartment, a fraction collector and the ChemStation (for LC 3D A.09.03) data system (Agilent, St-Laurent, QC, Canada). LC-MS analyses were performed on a Spectra System P4000 (Spectro Separation Products) equipped with a UV 2000 detector and a Finnigan LCQ DUO (ion trap) mass detector set up in Atmospheric Pressure Chemical Ionization (APCI) negative mode, controlled by the Xcaliber software version 1.2.

Absorbance spectra were acquired using an Agilent 8453 spectrophotometer equipped with a diode-array (Agilent, St-Laurent, QC, Canada). Measurements were done in a 1 cm quartz cuvette.

1.3.3 HPLC purification of the amyloid-beta (1-42) peptide ($A\beta_{1-42}$)

The purification of full length amyloid beta peptide ($A\beta_{1-42}$) was optimized after testing different columns such as Polymerex 100 Å (Phenomenex, Torrance, CA), Zorbax C8 (n-octane) 300 Å, Zorbax C18 (octadecyl silane) 80 Å and Zorbax CN (n-butyl cyano) 80 Å (Agilent, St-Laurent, QC, Canada). The trials were conducted with a gradient of acetonitrile/water or methanol/water under acidic or basic conditions. The additives used, trifluoroacetic acid or ammonium hydroxide, were selected to facilitate further LC-MS experiments, since they are compatible with the mass detector. The $A\beta_{1-42}$ was successfully purified with a 250 x 4.6 mm 5µ 300 Å C18 Extend column (Agilent, St-Laurent, QC, Canada). $A\beta_{1-42}$ was eluted using a gradient of 10% to 40.5% of solvent B in solvent A over 30 min at a flow rate of 1 ml/min. Solvent A composition was 5 mM NH_4OH in water and the solvent B composition was 5 mM NH_4OH in acetonitrile. The absorption spectrum was recorded at 215 nm. The column temperature was controlled at 25°C. Prior to injection, the $A\beta_{1-42}$ was dissolved to 4 mg/ml in an aqueous solution containing 3% NH_4OH. Under these conditions, the retention time of $A\beta_{1-42}$ was 15.3 min, as confirmed by LC-MS.

1.3.4 Abeta deaggregation

$A\beta_{1-42}$ (1 mg) was dissolved in 1 ml of 3% NH_4OH aqueous. The mixture was vortexed, sonicated 1 minute, aliquoted and lyophilized. The lyophilized aliquots were stored at -80°C.

1.3.5 CD analysis

The secondary structure of $A\beta_{1-42}$ was determined by circular dichroism (CD) spectroscopy and was expressed as an average of three accumulations measured at 25°C. The accumulations were recorded using a response time of 4 sec, a speed scan of 100 nm/sec and a bandwidth interval of 0.2 nm over the wavelength range of 195 to 260 nm. The stock solution of $A\beta_{1-42}$ was freshly prepared by dissolving deaggregated $A\beta_{1-42}$ (886.1 μM) in TFE. For each molecule tested, the stock solution was obtained by dissolving the molecule of interest, at the desired concentration, in a filtered solution of 40:60 v/v or 25:75 v/v TFE:100 mM potassium phosphate buffer at pH 7.4.

The final mixture (250 μl) analyzed by CD contained the potential ligand at various concentrations and the $A\beta_{1-42}$ (31.9 μM) in 25:75 or 40:60 (v/v) TFE:100 mM potassium phosphate buffer at pH 7.4. This mixture was transferred to a 1 mm-cuvette and incubated 5 min at 25°C prior to acquiring the CD scans. After the acquisition and blank subtraction, the CD data were transformed into mean residue ellipticity ($[\theta]\lambda$) in $deg \cdot cm^2/dmol$, according to the following equation:

$$[\theta]\lambda = (\theta\lambda) \cdot (MRW) / 10 \cdot l \cdot c \qquad \text{Eq 1}$$

Where θ corresponds to the measured ellipticity angle at wavelength λ (mdeg), MRW is the mean residue weight, i.e. the peptide molecular weight/number of amino acids (in dmol), l is the optical path length (cm), and c is the peptide concentration (g/ml).

The data were analyzed by the CD pro software package[56] which includes SELCON3[57], CONTIN/LL[58] and CDSSTR[59] methods. In addition, the data were also analyzed using the 208 nm[60] and 222 nm[61] absorptions, to facilitate the comparison of our results with some found in the literature. The equations employed to determine the α-helix percentage with θ_{208} and θ_{222} methods are given below. CD data were transformed in mean residue ellipticity ($[\theta]\lambda$) before using Equations 2 and 3.

$$\% \text{ α-helix}_{\theta 208} = ([\theta]_{208} - 4000/-37000) \times 100 \qquad \text{Eq 2}$$

$$\% \text{ α-helix}_{\theta 222} = ([\theta]_{222} - 3000/-39000) \times 100 \qquad \text{Eq 3}$$

1.3.6 KAD tripeptide **10** (Lys-Ala-Asp)

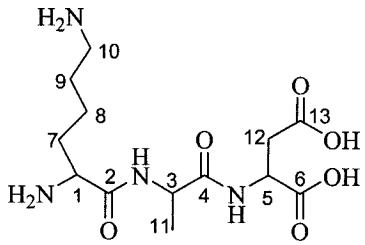

The Fmoc strategy was used to synthesize the tripeptide KAD (**10**) on solid support. The Wang resin (1.5 g) was initially swelled for 30 min in DMF. Unless indicated, all the solutions used were in DMF. Coupling of the C-terminus amino acid to the resin was performed at room temperature using the activated aspartic acid solution (15 ml) which contained Fmoc-Asp(Boc)-OH (0.34 M), DIPEA (0.68 M) and HATU (0.34 M). After 2

hours, the resin was washed several times with DMF and capped with pyridine (15 mL) containing acetic anhydride (0.34 M). Deprotection of the aspartic acid amino group was achieved using 25% piperidine (2 x 15 ml) for 3 and 20 min respectively. Again, the resin was washed several times with DMF. The coupling and the deprotection of the alanine and the lysine were achieved similarly but without the capping step. Fmoc-Ala-OH and Fmoc-Lys(Boc)-OH were used. After each coupling and deprotection a ninhydrin test (see next page) was performed to confirm completion of the reaction. Prior to the final cleavage, the peptide was washed with DCM many times to remove the DMF. The peptide was cleaved from the resin using 50% TFA in DCM (15 ml) for 1 hour. Finally, the peptide was precipitated using 8 volumes of diethylether. The tripeptide was purified by HPLC using a 250 x 4.6 mm Zorbax RP-AQ 5 μ 80 Å column (Agilent, St-Laurent, QC, Canada). Isocratic elution was achieved using 0.1% TFA in water at a flow rate of 1 ml/min. The column temperature was set to 45°C and the absorbance was recorded at 214 nm. The peptide **10** was obtained as a white powder (80.0 mg, 10% overall yield). **HPLC** ret. time: 3.5 min; **^{1}H NMR** (400 MHz, D_2O) δ 4.36 (t, 1H, J = 5.6 Hz, H-5), 4.22 (q, 1H, J = 7.2, H-3), 3.85 (t, 1H, J = 6.0 Hz, H-1), 2.84 (t, 2H, J = 7.6 Hz, H-10), 2.67 (d, J = 5.6 Hz, H-12), 1.76 (m, 2H, H-7), 1.55 (m, 2H, H-9), 1.30 (m, 2H, H-8), 1.24 (d, J = 7.2, 3H, H-11); **^{13}C NMR** (75 MHz, D_2O) δ 175.9 (C-6), 175.5 (C-13), 173.8 (C-4), 169.4 (C-2), 53.0 (C-1), 51.0 (C-5), 50.0 (C-3), 39.2(C-10), 37.1 (C-12), 30.6 (C-7), 26.6 (C-9), 21.3 (C-8), 16.7 (C-11); **LRMS** (LC-MS(ESI)): Calcd for $C_{13}H_{24}O_6N_4$ 332.17; Found 331.2 (M $-H^+$).

1.3.7 Bis(2,2,2-trifluoroethyl)malonate (**11**)

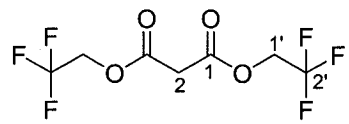

After dissolution of malonic acid (21.8 mM) in toluene (20 ml), 2,2,2-trifluoroethanol (135 mM) and sulfuric acid (8 drops) were added to the mixture which was refluxed at 90°C for 12 hours. The mixture was then washed three times with 10% sodium bicarbonate and one time with brine. The organic layer obtained was evaporated *in vacuo*. The product **11** was obtained as a yellowish oil (1.13 g, 20%). **^{1}H NMR**: (300 MHz, $CDCl_3$) δ 4.80 (q, 4H, J = 8.9 Hz, H-1'), 3.87 (s, 2H, H-2); **^{13}C NMR**: (75 MHz, $CDCl_3$) δ 165.29 (s), 123.84 (q, J = 366.3 Hz, C-2'), 61.18 (q, J = 47.1 Hz, C-1'), 40.43 (m, C-2); **LRMS** (ESI): Calcd for $C_7H_6F_6O_4$ 268.0170; Found: 267.0 ($M - H^+$).

1.3.8 Ninhydrin test

This test was carried out by adding two drops of ninhydrin (5% w/v in ethanol), one drop of phenol (4:1 w/v in ethanol) and one drop of potassium cyanide (20 μM) in pyridine, in a small glass test tube containing approximately 0.02 ml of the reaction mixture. The tube was then heated for 2-3 min using a heat gun with shaking. A positive test was revealed by color change, from yellow (protected amino acid) to a dark blue (free primary amine).

1.4 RESULTS AND DISCUSSION

1.4.1 Alzheimer's amyloid beta peptides

The amyloid beta peptide (Aβ) is the major component of the senile plaques found in the brain of patients with Alzheimer disease[62,63]. Amyloid beta is formed *in vivo* in a length varying from 39 to 43 amino acids, $A\beta_{1-40}$ being the most abundant and $A\beta_{1-42}$ being the predominant form found in Alzheimer's amyloid plaques. $A\beta_{1-42}$ shows the highest tendency to aggregate and is the most neurotoxic[64]. For these reasons, $A\beta_{1-42}$ was used in our investigations, in spite of the fact that it is more difficult to handle than the shorter Aβ peptides.

1.4.2 $A\beta_{1-42}$ purification

American Peptide Company sells $A\beta_{1-42}$ as >95% pure but only in very small amounts. Larger amounts of $A\beta_{1-42}$ were purchased from Service de Synthèse de Peptide de l'Est du Québec (Québec, QC, Canada) as a crude powder. Many HPLC columns and conditions were tested to purify crude $A\beta_{1-42}$. The main difficulty was related to the small pore size of most of the columns tested (80-100 Å) except for the Zorbax C8 and the C18 Extend which had a pore size of 300 Å. The molecular weight of $A\beta_{1-42}$, 4514.5 g/mol, was not considered initially in the choice of the column. Indeed it is well known that molecules having a molecular weight above 2000 g/mol must be purified using 300 Å-pore size columns[65]. The problem was solved by using the column Zorbax C18 Extend 300 Å.

Another difficulty encountered was related to the pH of the mobile phase, which is usually acidic. As the pH is lowered, $A\beta_{1-42}$ reaches its isoelectric point (5.2), a pH region where it easily aggregates[66,67]. Poor separation and resolution of $A\beta_{1-42}$ was observed under acidic conditions and the large peak obtained (Figure 10) is believed to contain aggregated peptides of various sizes. This second problem was solved by using basic conditions, i.e. using mobile phases buffered with 5 mM ammonium hydroxide.

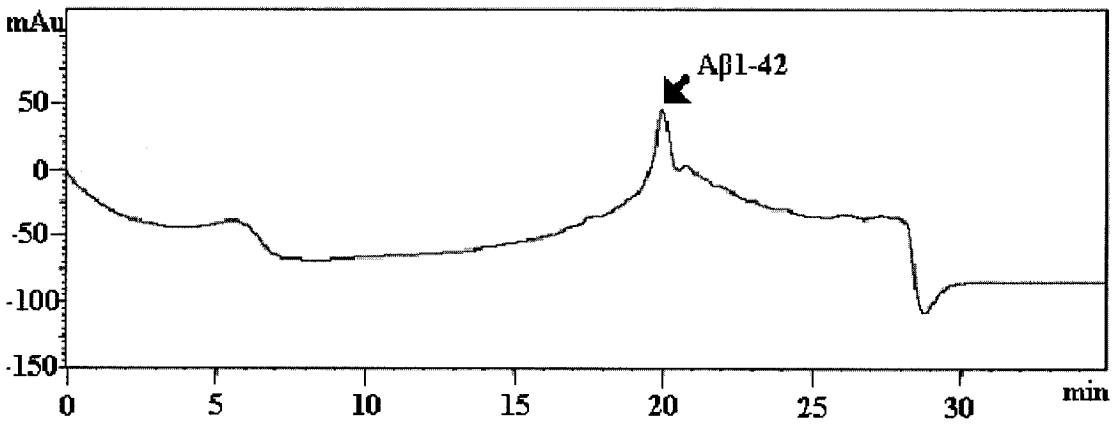

Figure 10 - Chromatogram of crude $A\beta_{1-42}$ (20 µl of 4 mg/ml in acetonitrile) acquired under acidic conditions. $A\beta_{1-42}$ was separated using a 80 Å Stable Bond C18 column with a gradient of 10 to 40.5% solvent B in solvent A over 30 min at a flow rate of 3 ml/min. The solvent A was 0.1% TFA in water at pH 3.0 and the solvent B was acetonitrile containing 0.1% TFA at pH 3.0. The column temperature was controlled at 25°C. Under these conditions monomeric $A\beta_{1-42}$ elutes at 20.0 min and its absorption is recorded at 214 nm.

Figure 11 shows the chromatogram of crude $A\beta_{1-42}$ purified by HPLC using a 300 Å C18 Extend column under basic conditions. Mobile phases used were aqueous ammonium hydroxide (5 mM) and acetonitrile containing ammonium hydroxide (5 mM). The chromatogram of crude $A\beta_{1-42}$ contains many unidentified impurities, which are likely to include chemicals used during the solid phase peptide synthesis, truncated peptides, and aggregated $A\beta_{1-42}$ peptides. The $A\beta_{1-42}$ peak was identified by LC-MS.

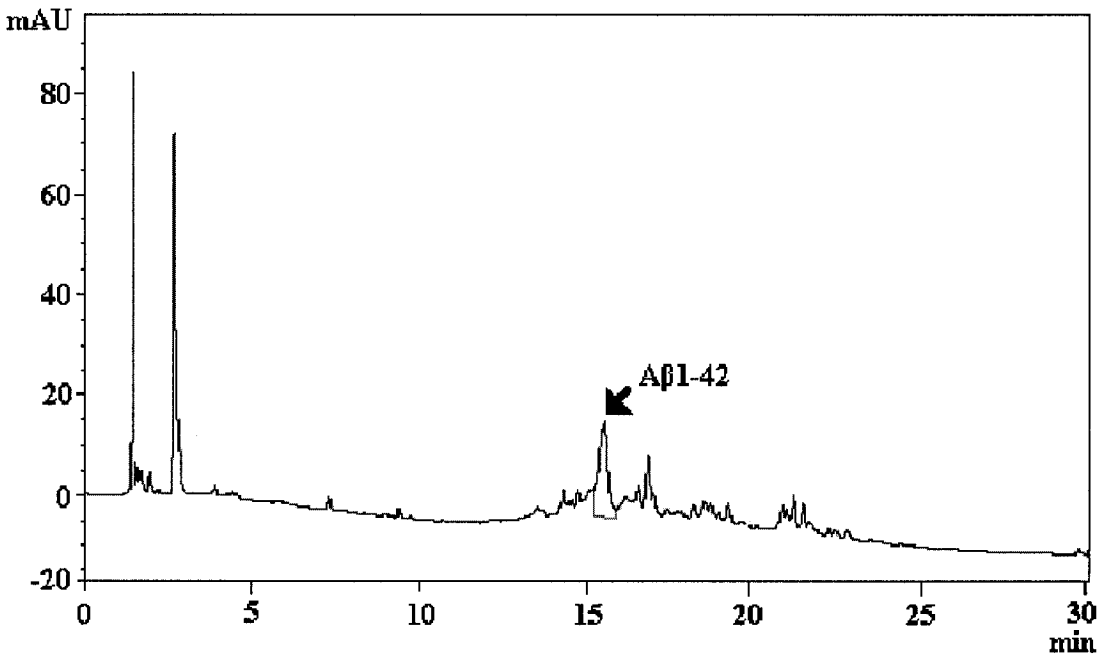

Figure 11 - Chromatogram of crude $A\beta_{1-42}$ (5 µl of 4 mg/ml in acetonitrile) eluted on a C18 300 Å Extend column under basic conditions. Separation was achieved with a gradient of 10 to 40.5% solvent B in solvent A over 30 min at a flow rate of 1 ml/min. The solvent A was aqueous ammonium hydroxide (5 mM) at pH 8.0 and the solvent B was acetonitrile containing ammonium hydroxide (5 mM) at pH 8.0. The column temperature was controlled at 25°C. $A\beta_{1-42}$ elutes at 15.3 min and its absorption is recorded at 214 nm.

Figure 12 next page shows the chromatogram of crude $A\beta_{1-42}$ (5 µl of 4 mg/ml) dissolved in 3% ammonium hydroxide solution, compared to that of $A\beta_{1-42}$ (5 µl of 4 mg/ml) dissolved in acetonitrile:water 15:85 (v/v). $A\beta_{1-42}$ dissolved under basic conditions shows a higher peak than $A\beta_{1-42}$ dissolved in acetonitrile:water 15:85 (v/v). This observation suggests that the aggregation of $A\beta_{1-42}$ may be prevented or partially reversed under basic conditions.

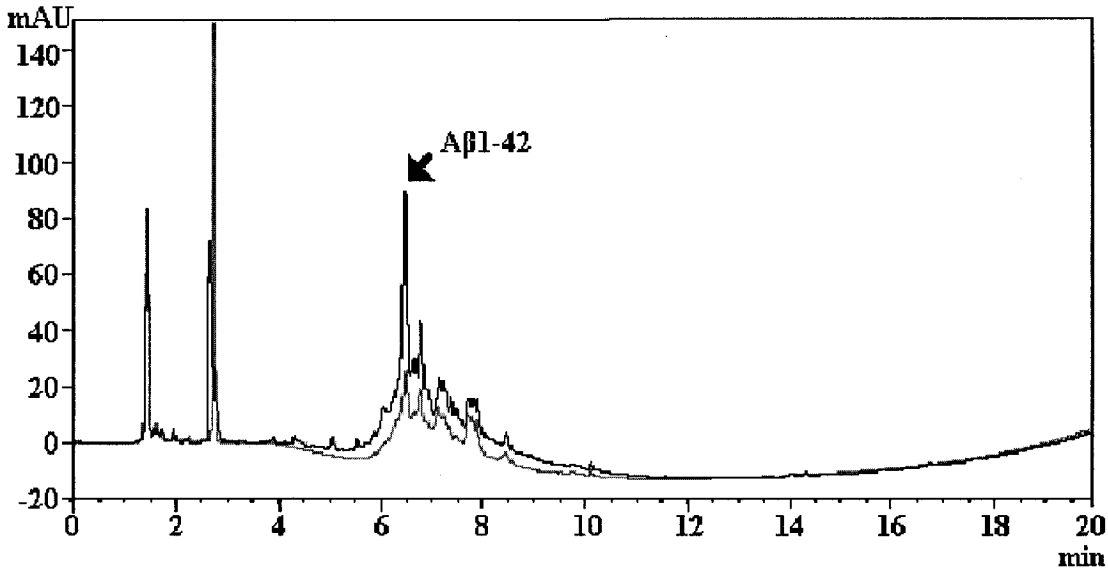

Figure 12 - Chromatogram of crude $A\beta_{1-42}$ (5 µl of 4 mg/ml) dissolved in aqueous ammonium hydroxide (5 mM) (black) versus $A\beta_{1-42}$ dissolved in acetonitrile:water 15:85 (grey). Separation was achieved using a C18 300 Å Extend column with a gradient of 10 to 100% solvent B in solvent A over 20 min at a flow rate of 1 ml/min. The solvent A was an aqueous ammonium hydroxide solution (5 mM) at pH 8.0 and the solvent B was acetonitrile containing ammonium hydroxide (5 mM) at pH 8.0. The column temperature was controlled at 25°C. $A\beta_{1-42}$ elutes at 6.3 min and its absorption is recorded at 215 nm.

1.4.3 Investigation of molecules **1-11** for their effects on the secondary structure of $A\beta_{1-42}$

The molecules presented in Figure 13 were tested by circular dichroism for their effect on the secondary structure of $A\beta_{1-42}$. Molecules **1** to **9** were synthesized by Dr. Samia Ait-Mohand in our laboratories. They were designed by basic modeling experiments using the NMR helical structure of $A\beta_{1-42}$ reported by Crescenzi *et al.*[68].

Kemp *et al.* have reported many capping molecules that favor helical peptides when covalently attached to the N-terminus (N-caps) or the C-terminus (C-caps) of the peptide[37]. We envisioned that the intermolecular version of these molecules may stabilize helical $A\beta_{1-42}$ if high enough concentrations are used to compensate for the intramolecular effect. One C-capping molecule (**8**) and one N-capping molecule (**9**) were synthesized by Dr. Ait-Mohand in order to test their effect on the secondary structure of $A\beta_{1-42}$. The synthetic protocol was adapted to allow a covalent link to be introduced to attach **8** and **9** together; however, formation of the link was synthetically problematic and was abandoned.

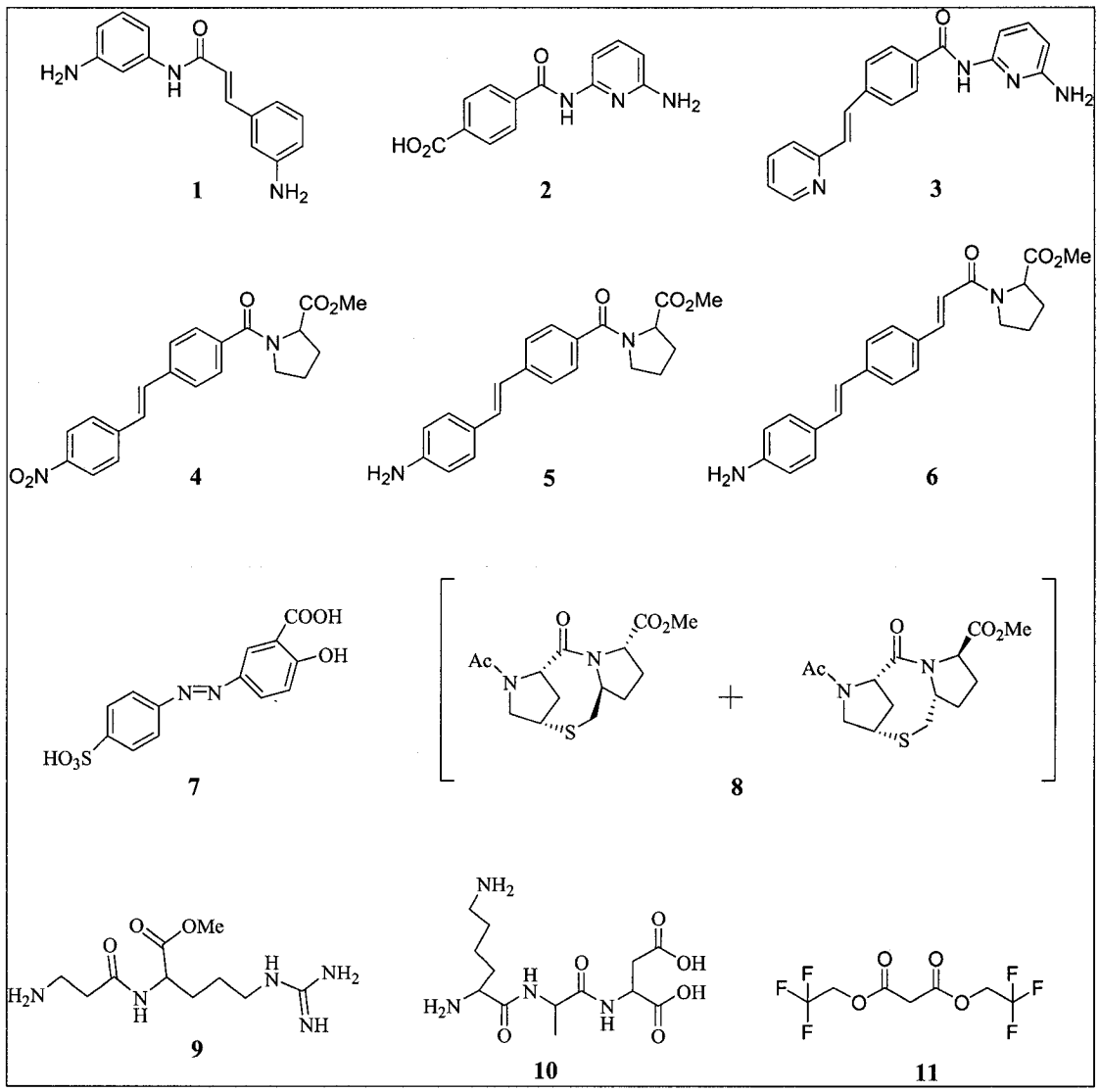

Figure 13 - Molecules tested for their effect on the conformation of $A\beta_{1-42}$.

Johansson and coworkers have reported that the tripeptide KAD (1 mM, Lys-Ala-Asp, **10**) increases the percentage α-helix of $A\beta_{12-28}$ (100 μM) by 5% in 40% aqueous 2,2,2-trifluoroethanol[69]. We synthesized this tripeptide (**10**) to test it on the full length $A\beta_{1-42}$. Initially, classical wet chemistry was employed to synthesize molecule **10**. Unfortunately,

the purification of the final product was not possible with the material available, since impurities co-eluted with the tripeptide on HPLC. On the other hand, the tripeptide was successfully synthesized when solid phase peptide synthesis was used (Scheme 1) starting from Fmoc-Asp(Boc)-OH, Fmoc-Ala-OH and Fmoc-Lys(Boc)-OH, where Fmoc is *N*-(9-fluorenylmethoxycarbonyl), Asp is aspartic acid, Boc is *N-(tert*-butoxycarbonyl), Ala is alanine and Lys is lysine. The first step was the coupling of the Fmoc-protected aspartic acid to the Wang resin using *N,N*-diisopropylethylamine (DIPEA) and *O*-(7-azabenzotriazol-1-yl)-*N,N,N',N'*-tetramethyluronium hexafluorophosphate (HATU). The coupling was monitored using the ninhydrin test. To avoid the formation of truncated peptides, unreacted resin was capped with a solution of acetic anhydride:pyridine 50:50 (v/v). After filtration to remove excess reagents, the Fmoc protecting group of the resin-attached aspartic acid was removed with piperidine. The second amino acid, alanine, was activated with DIPEA and HATU for coupling with the aspartate, followed by deprotection as described above. The last amino acid, lysine, was attached using the same conditions as for alanine. Finally, the tripeptide was cleaved from the resin and its side chain Boc protecting groups were removed using dichloromethane:trifluoroacetic acid 50:50 (v/v). The tripeptide was precipitated in ether, purified by HPLC and identified by LC-MS. The yield was 10% over 7 steps.

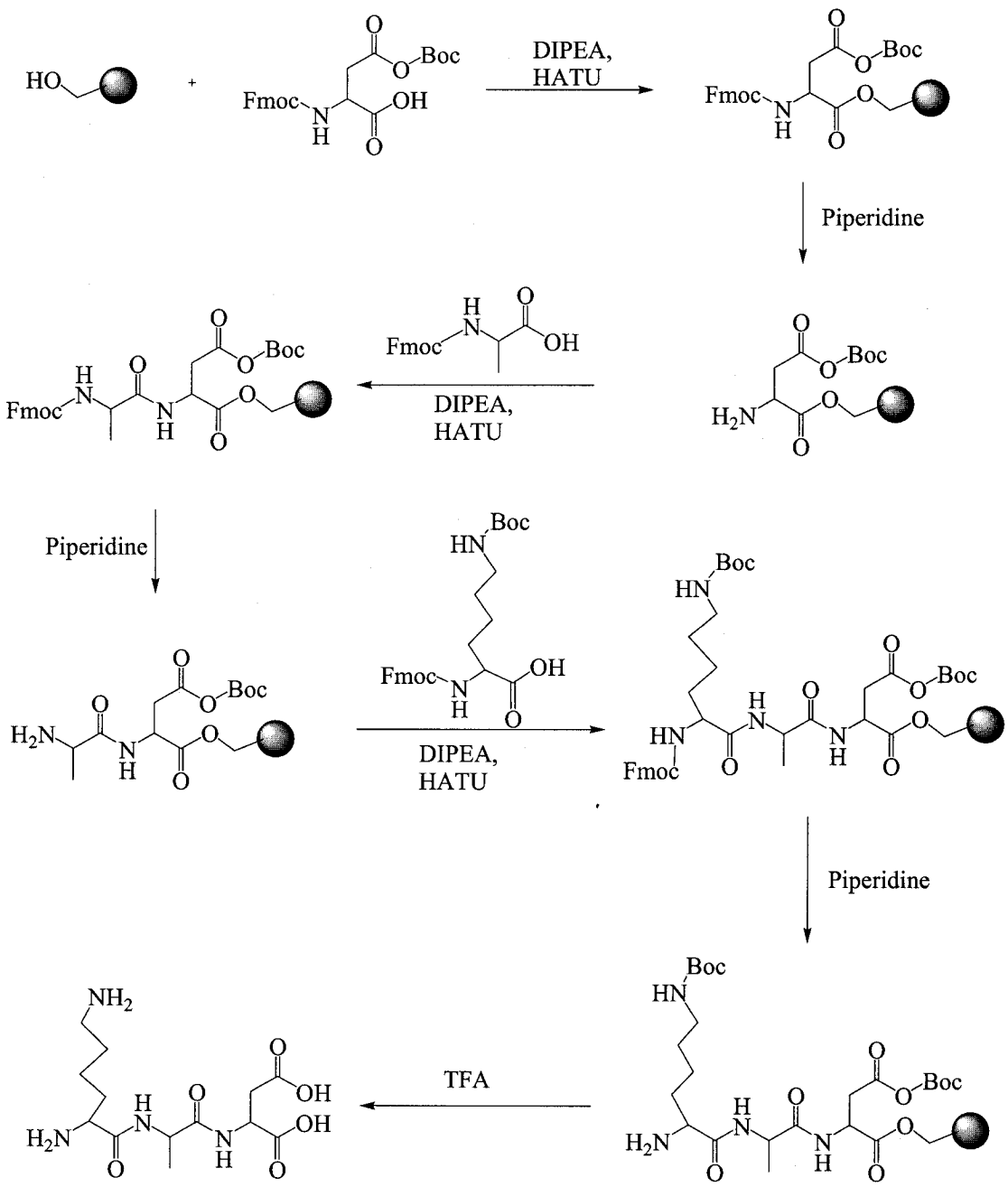

Scheme 1 - Solid phase synthesis of the KAD tripeptide (**10**).

Finally, bis(2,2,2-trifluoroethyl) malonate (**11**) was inspired from the fluorinated solvents 2,2,2-trifluoroethanol (TFE) and 1,1,1,3,3,3-hexafluoroisopropanol (HFIP), known for their ability to increase helical conformation of peptides in general[39]. The bis(2,2,2-

trifluoroethyl) malonate (**11**) was obtained by double esterification of malonic acid with TFE as shown on Scheme 2. The reaction was catalyzed by sulfuric acid (catalytic amount) in refluxing toluene and the yield was 20%. The fact that the boiling point of the TFE was inferior to the refluxing temperature may explain the low yield obtained.

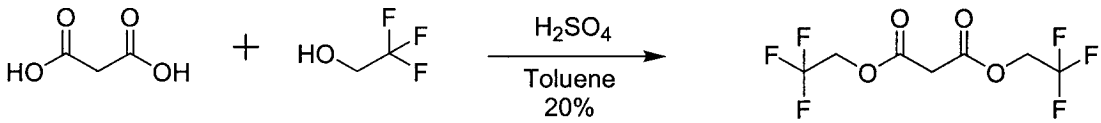

Scheme 2 - Synthesis of bis(2,2,2-trifluoroethyl) malonate (**11**).

1.4.4 Circular dichroism (CD) analyses

Circular dichroism (CD) and Fourrier transform infrared spectroscopy (FTIR) are two techniques commonly used to predict protein and peptide secondary structures when they cannot be obtained by X-ray crystallography or nuclear magnetic resonance. CD and FTIR are ideal for quick screening of ligands and conditions that may affect protein and peptide secondary structures. Because the critical concentration for $A\beta_{1-42}$ aggregation is 40 μM[51], our CD studies with $A\beta_{1-42}$ were carried at 31.9 μM. In this thesis, CD was chosen over FTIR for the determination of peptide secondary structure. This choice was based on the concentration of $A\beta_{1-42}$ tested, since the peptide range concentration recommended for CD and FTIR analyses are 0.01-0.10 mM and 0.5-2.0 mM respectively.[70] FTIR also requires the use of more expensive deuterated buffers.

1.4.4.1 Methods used for the analysis of CD data

All the methods reported for the prediction of the secondary structure of peptides and proteins assume that the far-UV CD data (190-260 nm) can be expressed as a linear combination of the different secondary structures plus a noise constant. The least squares method was the first method developed to predict secondary structures. In this method, spectra of polypeptides with known conformations are used to build a calibration curve. Well known approaches using the least squares method are θ_{208} and θ_{222}. After this first generation of CD data analysis tools, a wide number of protein conformations were rapidly determined and larger databases of spectra (reference set) were used to improve the secondary structure prediction methods. The reference set was deconvoluted to a basis spectrum (CD curve) for each of the secondary structures in their pure form. Therefore, the basis spectra have replaced the single polypeptide spectrum as the standard in CD calibration curve. LINCOMB is an example of a method using deconvoluted reference spectra in its standard calibration curve. In addition to the least squares method, singular value decomposition and convex constraint analysis are currently used to deconvolute reference sets of protein structures. Figure 14 shows an example of basis spectrum of common secondary structures obtained with the least squares method.

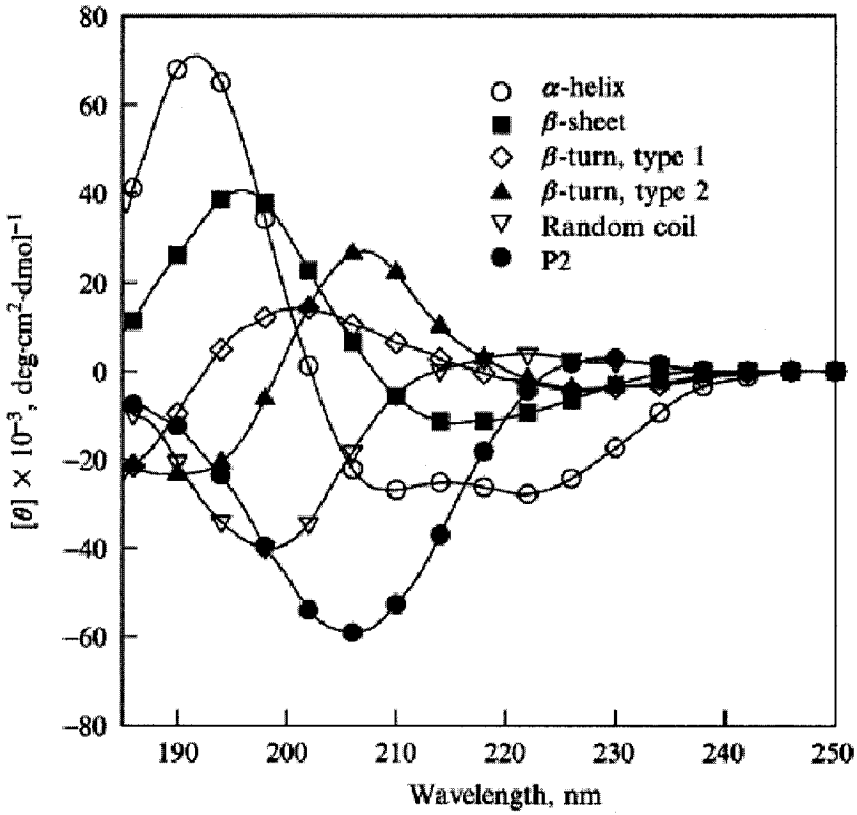

Figure 14 – Basis spectra for the most common secondary structures found in proteins, calculated by deconvolution of protein reference sets using the least squares method. Figure extracted from Greenfield[71].

The basis spectrum obtained after deconvolution may vary significantly depending on the proteins selected in the reference set. To overcome this difficulty, new methods have been developed where the reference set includes only proteins having similar characteristics to the protein of interest. Those modern methods include ridge regression analysis (CONTIN), singular value decomposition with variable selection (CDSSTR), self-consistent analysis (SELCON) and neutral network (K2D)[72]. Table 4 summarizes the prediction methods commonly used, their recommended wavelength range, the effect of truncated data on the secondary structure prediction, and the suggested utilization.

LINCOMB, θ_{208} and θ_{222} are especially recommended for determination of relative changes in the secondary structure, but they generally perform poor predictions of β-sheets and β-turns. Moreover, θ_{208} and θ_{222} methods overestimate α-helix content, due to the fact that only two types of structures are considered, namely α-helix and β-sheet. CDSSTR and CONTIN are recommended for determination of polypeptide conformations; however, the first one is highly sensitive to truncated data. Finally, SELCON performs very good predictions for all secondary structures, and performs well with truncated data. It is recommended for secondary structure analysis of globular proteins, whereas it is not optimized for polypeptides with a high β-pleated sheet content[34,54].

All these methods may be used with different protein reference sets in order to generate basis spectra which are then utilized to predict secondary structures. Consequently, it is very difficult to compare results determined by different methods. To overcome this lack of consistency, the CD data presented in this thesis were treated with the CD pro software[40], which includes modified version of SELCON3, CONTIN/LL and CDSSTR. The first modification is the use of a common protein reference set which includes the reference sets of SELCON3, CONTIN/LL and CDSSTR. Moreover, the three methods of the CD pro software used the same secondary structures: regular α-helix, distorted α-helix, regular β-strand, distorted β-strand, turn and unordered structure. For simplicity, the regular and the distorted α-helices were combined for analysis. The same is also true for the regular and the distorted β-strands. They were respectively renamed α-helix and β-sheet. Furthermore, the α-helix content was also determined using single wavelength methods, θ_{208} and θ_{222}, to facilitate the comparison of our results with some of the literature.

Table 3 - Comparison of methods used to analyze circular dichroism data

Methods	λ range (nm)	**Evaluation of secondary structures using truncated data (240-200 nm)**[a]			Suggested uses
		helix	sheet	turn	
θ_{208}, θ_{222}	208-240	***	**	*	▪ Quantification of secondary structure changes
LINCOMB	178-240	***	*	*	▪ Estimation of polypeptide conformations ▪ Quantification of secondary structure changes
SELCON	178-260	***	**	**	▪ Estimation of globular protein conformations ▪ **Not** recommended for estimation of polypeptide conformation with high content in β-pleated sheets
CONTIN	178-260	***	**	**	▪ Estimation of polypeptide conformations
CDSSTR	178-260	N/A[b]	N/A	N/A	▪ Estimation of polypeptide conformations ▪ **Not** recommended for truncated data
K2D	178-260	***	***	N/A	▪ Estimation of peptide conformations

[a] Poor (*), correlation coefficient ≤ 0.5; Good (**), correlation coefficient 0.5-0.75; Excellent(***), correlation coefficient ≥ 0.75. [b] N/A = Not available

All the CD data obtained for the molecules investigated in this present thesis were analyzed with the five methods presented above (SELCON3[41], CONTIN/LL[42], CDSSTR[43], θ_{208}[44] and θ_{222}[45]) for comparison and improved reliability. These methods were all suitable to monitor the conformational changes of $A\beta_{1-42}$ in the presence of different ligands[53]. For clarity, only the results obtained with CONTIN/LL are listed in this thesis. This method was selected because it is less sensitive to truncated data. It should be kept in mind that

the goal of this project is to determine changes in $A\beta_{1-42}$ secondary structure and not its absolute conformation.

1.4.4.2 Effect of NH_4OH, TFE and NaOH on the deaggregation of $A\beta_{1-42}$

Upon its storage in solution or as a solid, $A\beta_{1-42}$ is known to slowly aggregate and eventually form fibrils. The various levels of aggregation in different samples may lead to inconsistencies in the results[73,74]. A deaggregation protocol was established and performed prior to each experiment to ensure a reliable monomeric $A\beta_{1-42}$ content. The deaggregation protocol tested consisted of deaggregation of $A\beta_{1-42}$ in NaOH, NH_4OH or TFA (10 min at room temperature), followed by lyophilization and solubilization in TFE. The percentage of each secondary element was determined by circular dichroism (Figure 15). The presence of α-helices is revealed by negative cotton effect at 212 and 222 nm. The exact percentages of secondary elements were determined using CD pro software. When aqueous sodium hydroxide (10 mM) was used to deaggregate $A\beta_{1-42}$, the ratio of α-helix:β-sheet:β-turn:unordered obtained in potassium phosphate buffer containing 40% TFE was 32:18:22:29 (Figure 15). The secondary structure ratio of $A\beta_{1-42}$ shifted to 36:15:22:27 and 35:18:21:27 when 3% ammonium hydroxide and 1% trifluoroacetic acid were used instead of NaOH, respectively. The secondary structure ratios under these conditions are not considered significantly different (<5%) (Table 4). However, NH_4OH was chosen to deaggregate $A\beta_{1-42}$ prior to all experiments because of its ease of removal and its compatibility with the HPLC purification. HPLC analysis suggests that NH_4OH may increase the proportion of monomeric $A\beta_{1-42}$. Moreover, the solubilization of $A\beta_{1-42}$ in TFE was easier after NH_4OH deaggregation compared to NaOH or TFA deaggregation.

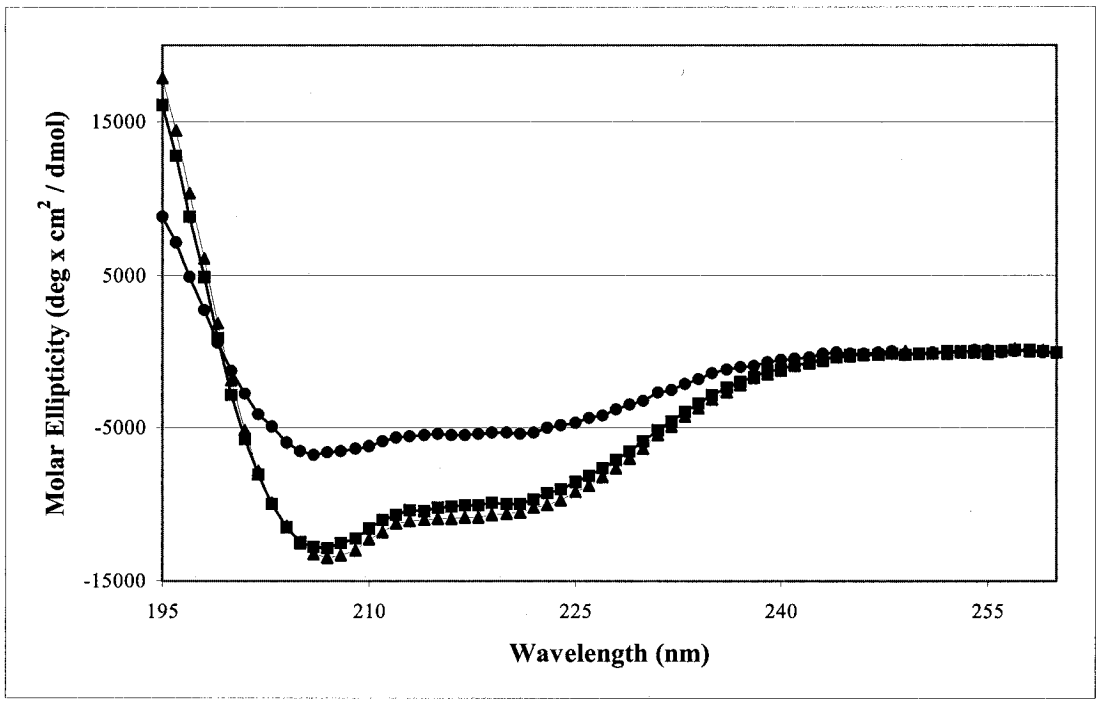

Figure 15 – CD spectrum of $A\beta_{1-42}$ (31.9 μM) after deaggregation with NH_4OH (●), NaOH (■) and TFA (▲). Spectra acquired in 40:60 (v/v) TFE:potassium phosphate buffer (100 mM, pH 7.4) at 25°C.

Table 4- Effect of the NH_4OH, TFA and NaOH deaggregation procedures on the secondary structure of $A\beta_{1-42}$ (31.9 μM) in 40:60 (v/v) TFE:potassium phosphate buffer (100 mM, pH 7.4) at 25°C.

Deaggregation agent	Secondary Structure Percentage (%)							
	α-Helix[a]		β-Sheet[b]		Turn		Unordered	
NH_4OH	31.8	± 0.9	17.9	± 0.7	21.9	± 0	28.6	± 0.2
TFA	36.0	± 1	14.8	± 0.1	21.9	± 0.2	27.4	± 0.8
NaOH	35.1	± 1	18.7	± 2	21.3	± 0.6	26.9	± 0.4

[a] Sum of regular and distorted α-helix
[b] Sum of regular and distorted β-strand

1.4.4.3 Effect of TFE on the conformation of $A\beta_{1-42}$

In order to confirm the correlation between the conformation of $A\beta_{1-42}$ obtained under our conditions (purification and deaggregation) and the ones published in the literature, the conformation of $A\beta_{1-42}$ in various percentages of buffered TFE was determined by circular dichroism (Figure 16). The results are summarized on Figure 5. As expected, the helical content of $A\beta_{1-42}$ increases as the concentration of TFE is raised, whereas the β-sheet and β-turn contents decrease[75].

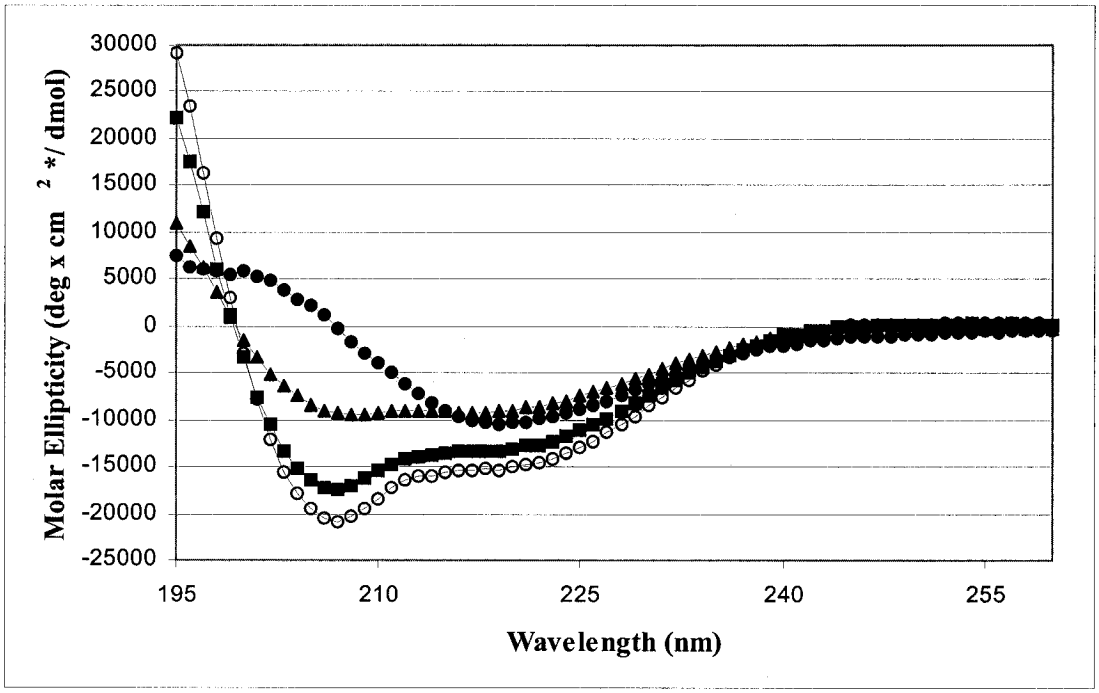

Figure 16 - CD spectrum of $A\beta_{1-42}$ (31.9 μM) in 15% (●), 25% (▲), 40% (■) and 80% (○) buffered TFE (100 mM potassium phosphate at pH 7.4 and 25°C).

Table 5- Effect of 15%, 25%, 40% and 80% TFE on the secondary structure of $A\beta_{1-42}$ (31.9 μM) in potassium phosphate buffer (100 mM, pH 7.4) at 25°C.

Percentage of TFA in buffer	Secondary Structure Percentage (%)							
	α-Helix[a]		β-Sheet[b]		Turn		Unordered	
15%	5.60	± 0.2	43.7	± 0.4	22.1	± 0.7	28.7	± 0.1
25%	23.5	± 0.2	24.7	± 0.3	22.2	± 0.1	29.7	± 0.2
40%	33.1	± 3	18.5	± 2	20.3	± 0.7	28.2	± 0.7
80%	52.3	± 3	6.90	± 2	14.2	± 0.9	26.5	± 0.2

[a] Sum of regular and distorted α-helix
[b] Sum of regular and distorted β-strand

1.4.4.4 Effect of synthetic molecules 1-11 on the secondary structure of $A\beta_{1-42}$

The effect of molecule **1** on the conformation of $A\beta_{1-42}$ (31.9 μM) was determined by CD (Figure 17) using 40% TFE in potassium phosphate buffer (100 mM, pH 7.4). When compared to a control experiment, molecule **1** (400 mM) did not significantly affect the conformation of $A\beta_{1-42}$. The secondary structure remained (within 5%) at 33% helix, 19% β-sheet, 20% β-turn and 28% unordered (Table 6).

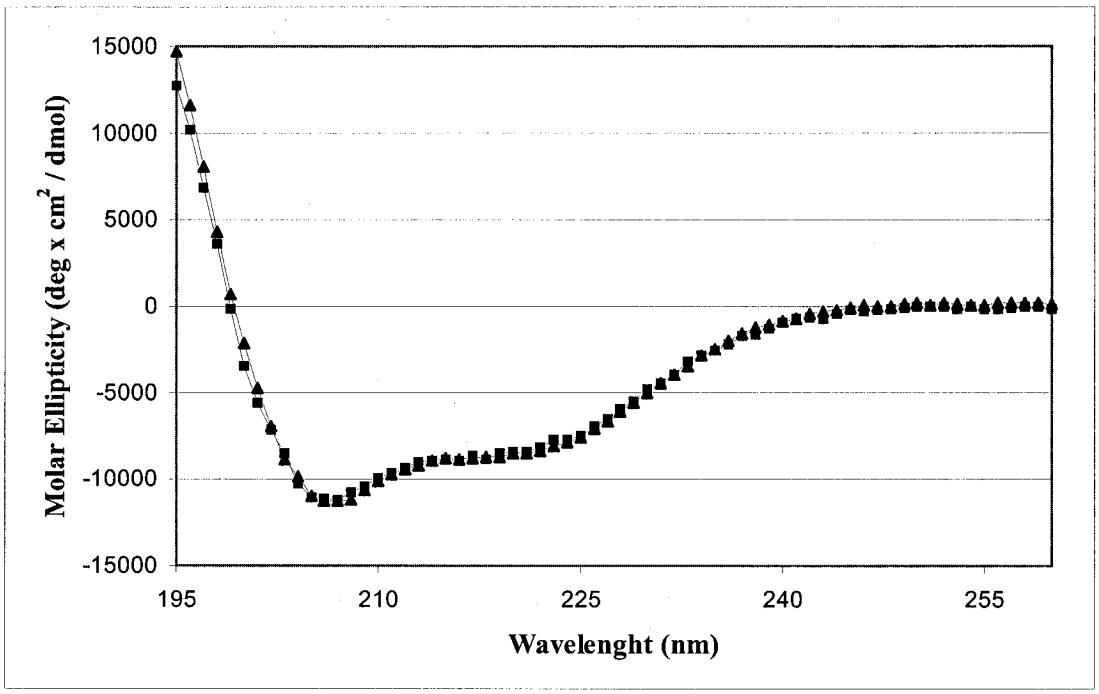

Figure 17 - CD spectrum of $A\beta_{1-42}$ (31.9 μM) with (▲) and without (■) molecule 1 (400 mM). Results obtained in 40:60 TFE:potassium phosphate buffer (100 mM, pH 7.4) at 25°C.

Table 6- Effect of molecules **1**, **2**, **3**, **4**, **5**, **6**, **7** and **11** (each at 400 mM) on the secondary structure of $A\beta_{1-42}$ (31.9 μM) in 40:60 (v/v) TFE:potassium phosphate buffer (100 mM, pH 7.4). The temperature was controlled at 25°C.

Sample	Secondary Structure Percentage (%)							
	α-Helix[a]		β-Sheet[b]		Turn		Unordered	
Abeta	33.1	± 3	18.5	± 2	20.3	± 0.7	28.2	± 0.7
Abeta + (**1**)	32.9	± 0.4	17.8	± 0.6	22.8	± 0.1	26.3	± 0.2
Abeta + (**2**)	38.4	± 0.6	15.8	± 0.1	19.3	± 2	26.7	± 2
Abeta + (**3**)	27.9	± 0.2	20.5	± 0.9	20.5	± 0.4	31.2	± 2
Abeta + (**4**)	36.0	± 0.9	15.2	± 0.5	22.1	± 0.2	26.8	± 0.6
Abeta + (**5**)	28.4	± 0.9	21.6	± 0.6	20.2	± 0.3	29.9	± 1
Abeta + (**6**)	35.9	± 3	16.1	± 1	22.3	± 0	25.7	± 1
Abeta + (**7**)	31.3	± 0.2	19.3	± 0.9	20.7	± 0.4	28.8	± 0.7
Abeta + (**11**)	30.1	± 0.5	19.7	± 0.2	20.7	± 0.6	29.6	± 0.3

[a] Sum of regular and distorted α-helix
[b] Sum of regular and distorted β-strand

The effect of molecules **2**, **4**, **5**, **6** and **7** on the conformation of $A\beta_{1-42}$ (31.9 μM) was determined by circular dichroism in potassium phosphate buffer (100 mM at pH 7.4), containing 40% or 25% TFE (Tables 6 and 7). Compared to a control experiments, addition of molecules (400 mM) did not significantly affect the conformation of $A\beta_{1-42}$ (<5%). The molecules were not tested at higher concentrations because of the significant noise below 200 nm.

Table 7- Effect of molecules **2**, **4**, **5**, **6** and **7** (each at 400 mM) on the secondary structure of $A\beta_{1-42}$ (31.9 μM) in 25:75 (v/v) TFE:potassium phosphate buffer (100 mM, pH 7.4). The temperature was controlled at 25°C.

Sample	Secondary Structure Percentage (%)							
	α-Helix[a]		β-Sheet[b]		Turn		Unordered	
Abeta	21.0	± 2	27.2	± 2	22.7	± 0.5	29.3	± 0.4
Abeta + (**2**)	15.5	± 4	29.6	± 1	23.6	± 1	31.3	± 2
Abeta + (**4**)	22.6	± 0,5	25.8	± 0.7	21.6	± 0.2	30.1	± 0.1
Abeta + (**5**)	22.4	n/a	25.1	n/a	22.3	n/a	30.3	n/a
Abeta + (**6**)	21.1	± 0.3	25.3	± 0.4	20.5	± 0.3	33.2	± 0.4
Abeta + (**7**)	17.7	± 3	29.7	± 2	22.7	± 0.8	29.9	± 1

n/a = experiment not performed in duplicate
[a] Sum of regular and distorted α-helix
[b] Sum of regular and distorted β-strand

The effect of molecules **3** and **11** (400 mM) on the conformation of $A\beta_{1-42}$ (31.9 μM) was determined by CD (Table 6) using 40% TFE in potassium phosphate buffer (100 mM, at pH 7.4). Compared to the control experiment, neither molecule significantly affected the conformation of $A\beta_{1-42}$ (<5%).

The effect of molecule **8** on the conformation of $A\beta_{1-42}$ (31.9 μM) was determined by CD in potassium phosphate buffer (100 mM, at pH 7.4) containing 40% TFE. Compared to the control experiment lacking **8**, addition of **8** (204 μM) did not significantly affect the conformation of $A\beta_{1-42}$ (Table 8). On the other hand, when **8** was tested at 612 μM, the α-helix percentage significantly dropped to 24% (Table 8). This variation in the α-helix content was attributed to insoluble aggregates and/or significant noise below 205 nm.

Table 8- Effect of molecules **8** and **9** on the secondary structure of $A\beta_{1-42}$ (31.9 μM) in 60:40 (v/v) TFE:potassium phosphate buffer (100 mM, pH 7.4). The temperature was controlled at 25°C.

Sample	Secondary Structure Percentage (%)							
	α-Helix[a]		β-Sheet[b]		Turn		Unordered	
Abeta	30.6	± 2	21.6	± 0.9	19.6	± 0.3	28.3	± 0.7
Abeta + (**8**) 204 uM	31.8	± 2	24.2	± 2	17.1	± 0.9	27.1	± 0.7
Abeta + (**8**) 612 uM	23.6	± 0.2	25.6	± 0.6	20.3	± 1	30.6	± 0.4
Abeta + (**9**) 1,2 mM	26.8	± 4	25.3	± 2	20.1	± 1	27.9	± 2
Abeta + (**9**) 2,6 mM	33.3	± 0.1	23.9	± 1	16.7	± 1	26.2	± 0.1

[a] Sum of regular and distorted α-helix
[b] Sum of regular and distorted β-strand

The effect of molecule **9** on the conformation of $A\beta_{1-42}$ (31.9 μM) was determined by CD in potassium phosphate buffer (100 mM, at pH 7.4) containing 40% TFE. Compared to the control experiment, molecule **9** (1.2 or 2.6 mM) did not significantly affect the secondary structure of $A\beta_{1-42}$ (<5%) (Table 8).

The secondary structure of $A\beta_{1-42}$ was determined in the presence of 1, 2, 3, 4, 5, 6, 8 and 10 mM of **10** in 40% buffered TFE. The results obtained for the concentrations 6 to 10 mM were too noisy for further analysis. When **10** was tested at 0, 1, 2, 3, 4 and 5 mM the

percentage of α-helix increased slightly (31, 31, 32, 29, 36, and 40 respectively), whereas the percentage of β-sheet decreased slightly (19, 18, 18, 18, 18, and 16 respectively) and the β-turn also diminished (22, 22, 22, 23, 18, and 15 respectively) (Table 9).

This rise in helix content observed in the presence of increasing amount of KAD (**10**) was however attributed to the huge amount of noise observed below 200 nm at higher concentrations. Thus, when the noisy section of the spectra (190-200 nm) was truncated, the amounts of α-helix determined for $A\beta_{1-42}$ in the presence of various concentrations of **10** were not significantly different (Table 9).

Table 9- Effect of molecules **10** (1, 2, 3, 4 and 5 mM) on the secondary structure of $A\beta_{1-42}$ (31.9 μM) in 60:40 (v/v) TFE:potassium phosphate buffer (100 mM, pH 7.4). The temperature was controlled at 25°C.

Sample	**Secondary Structure Percentage (%)** (calculated from 190-200 nm)							
	α-Helix[a]		β-Sheet[b]		Turn		Unordered	
Abeta	30.8	± 0.6	18.7	± 0.5	22.2	± 0.1	28.3	± 0.2
Abeta + 1 mM	30.8	± 0.4	18.3	± 0.5	22.0	± 0.1	29.0	± 0.4
Abeta + 2 mM	31.6	± 0.4	17.9	± 0.5	21.9	± 0.1	28.6	± 0.1
Abeta + 3 mM	28.7	± 2	20.2	± 2	22.3	± 0.3	29.0	± 0.4
Abeta + 4 mM	36.2	± 0.8	17.2	± 1	17.5	± 0.2	29.2	± 0.6
Abeta + 5 mM	39.5	± 0.8	15.5	± 0	16.4	± 1	28.7	± 0.5
	Secondary Structure Percentage (%) (calculated from 200 to 206 nm)							
Abeta	30.0	± 0.7	20.3	± 0.6	21.8	± 0.1	28.0	± 0.1
Abeta + 1 mM	29.9	± 0.1	19.6	± 0.4	21.8	± 0	28.8	± 0.4
Abeta + 2 mM	31.2	± 0.1	19.7	± 0.2	21.3	± 0.1	28.0	± 0.1
Abeta + 3 mM	27.8	± 2	21.8	± 1	22.0	± 0.4	28.5	± 0.1
Abeta + 4 mM	32.6	± 1	18.2	± 0.7	20.6	± 0.3	28.6	± 0.2
Abeta + 5 mM	34.7	± 2	20.3	± 0.6	21.8	± 0.1	28.0	± 0.1

[a] Sum of regular and distorted α-helix
[b] Sum of regular and distorted β-strand

1.4.4.5 Effect of selected molecules commercially available on the secondary structure of $A\beta_{1-42}$

Two additional molecules were tested by CD to determine their effect on the structure of $A\beta_{1-42}$. Sulfalazine was tested because it is used as a starting material in the synthesis of molecule **3**. The conformation of $A\beta_{1-42}$ was determined in potassium phosphate buffer (100 mM at pH 7.4) containing 40% TFE. The addition of sulfalazine (400 mM) did not significantly affect the conformation of $A\beta_{1-42}$ (<5%)(Table 10).

The second commercial molecule tested, Congo red, is a well-known inhibitor of Aβ peptide aggregation. It was envisaged that it may do so by shifting the conformational equilibrium towards helical $A\beta_{1-42}$. Congo red was tested in 25% buffered TFE. Addition of Congo red (10 and 100 μM), did not significantly affect the conformation of $A\beta_{1-42}$ (within 5%) (Table 10).

Table 10 - Secondary structure percentage of $A\beta_{1-42}$ in the presence of sulfalazine (400mM) and Congo red (CR) (10 and 100 μM) determined in 25% TFE in potassium phosphate buffer (100 mM at pH 7.4). The temperature was controlled at 25°C.

Sample	Secondary Structure Percentage (%)							
	α-Helix[a]		β-Sheet[b]		Turn		Unordered	
Abeta	16.7	± 0.5	33.3	± 2	25.0	± 0.9	24.9	± 2
Abeta + CR 10 mM	19.4	± 0.6	29.8	± 0.4	25.2	± 0.1	25.6	± 0.3
Abeta	27.3	± 3	21.5	± 5	23.1	± 0.2	28.2	± 2
Abeta + CR 100 mM	28.6	± 4	21.5	± 4	23.2	± 0.8	26.6	± 0.6
Abeta + sulfazine (400 mM)	35.5	± 2	15.1	± 0.8	21.7	± 0.7	27.7	± 1

[a] Sum of regular and distorted α-helix
[b] Sum of regular and distorted β-strand

1.5 CONCLUSION

In summary, we have developed a protocol to deaggregate and purify $A\beta_{1-42}$. We have also confirmed that TFE increases the helical content of $A\beta_{1-42}$. Overall, of all the molecules tested here, none have shown any significant effect on the conformation of $A\beta_{1-42}$. The strategy adopted here is not very convenient for the screening of molecules. Virtual screening (docking) of molecules designed will be a good complementary strategy, since it could predict the energy of binding between helical structure of $A\beta_{1-42}$ and the ligands.

1.6 REFERENCES

[1] J. Koolman, Colors atlas of biochemistry. 2nd Ed., Thieme, New-York, 2005, pp 467.

[2] P.Y. Chou, G.D. Fasman, Conformational parameters for amino acids in helical, beta-sheet, and random coil regions calculated from proteins. *Biochemistry*, 1974, 13, 211-222.

[3] N. Sewald, H.-D. Jakubke, Peptides: Chemistry and Biology. Wiley-VCH, 2002, pp 562.

[4] H.F. Gilbert, Basic concepts in biochemistry: a student's survival guide. 2nd Ed., McGraw-Hill, 2000, pp 331.

[5] R. A. Copeland, Enzymes: A practical introduction to structure, mechanism and data analysis. end Ed., Willey, New-York, 2000, pp 397.

[6] V. W. Rodwell, P.J. Kennelly, Proteins: Higher orders of structure. 26th Ed., McGraw-Hill, 2003, pp 623.

[7] S. Futaki, T. Kiwada, Y. Sugiura, Control of peptide structure and recognition by Fe(III)-induced helix destabilization. *J. Am. Chem. Soc.*, 2004, 126, 15762-15769.

[8] R.L. Beyer, H.N. Hoang, T.G. Appleton, D.P. Fairlie, Metal clips induce folding of a short unstructured peptide into an alpha-helix via turn conformations in water. Kinetic versus thermodynamic products. *J. Am. Chem. Soc.*, 2004, 126, 15096-15105.

[9] N.E. Shepherd, H.N. Hoang, G. Abbenante, D.P. Fairlie, Single turn peptide alpha helices with exceptional stability in water. *J. Am. Chem. Soc.*, 2005, 127, 2974-2983.

[10] J.P. Schneider, W.F. DeGrado, The design of efficient α-helical c-capping auxiliaries. *J. Am. Chem. Soc.*, 1998, 120, 2764-2767.

[11] W. Maison, E. Arce, P. Renold, R.J. Kennedy, D.S. Kemp, Optimal N-caps for N-terminal helical templates: effects of changes in H-bonding efficiency and charge. *J. Am. Chem. Soc.*, 2001, 123, 10245-10254.

[12] S. Hanessian, G. Papeo, K. Fettis, E. Therrien, M.T. PhanViet, Synthesis of 3_{10}-helix-inducing constrained analogues of L-proline. *J. Org. Chem.*, 2004, 69, 4891-4899.

[13] B. Heitmann, G.E. Job, R.J. Kennedy, S.M. Walker, D.S. Kemp, Water-solubilized, cap-stabilized, helical polyalanines: calibration standards for NMR and CD analyses. *J. Am. Chem. Soc.*, 2005, 127, 1690-1704.

[14] Y. Maeda, T. Nakagawa, Y. Kuroda, Oligopeptide-mediated helix stabilization of model peptides in aqueous solution. *J. Pept. Sci.*, 2003, 9, 106-113.

[15] F.D. Sonnichsen, J.E. Van Eyk, R.S. Hodges, B.D. Sykes, Effect of trifluoroethanol on protein secondary structure: an NMR and CD study using a synthetic actin peptide. *Biochemistry*, 1992, 31, 8790-8798.

[16] M. Fioroni, M.D. Diaz, K. Burger, S. Berger S., Solvation phenomena of a tetrapeptide in water/trifluoroethanol and water/ethanol mixtures: a diffusion NMR, intermolecular NOE, and molecular dynamics study. *J. Am. Chem. Soc.*, 2002, 124, 7737-7744.

[17] D. Roccatano, G. Colombo, M. Fioroni, A.E. Mark, Mechanism by which 2,2,2-trifluoroethanol/water mixture stabilize secondary-structure formation in peptides: A molecular dynamics study. *Proc. Natl. Acad. Sci. U S A.*, 2002, 99, 12179-112184.

[18] A. Starzyk, W. Barber-Armstrong, M. Sridharan, S.M. Decatur, Spectroscopic evidence for backbone desolvation of helical peptides by 2,2,2-trifluoroethanol: an isotope-edited FTIR study. *Biochemistry,* 2005, 44, 369-376.

[19] For review see: D.J. Selkoe, Folding proteins in fatal ways. *Nature*, 2003, 426, 900-904.

[20] For review see: L.C. Serpell, M. Sunde, C.C. f. Blake, The molecular basis of amyloidosis. *Cell. Mol. Life Sci.*, 1997, 53, 871-887.

[21] T.R Appel, S. Richter, R.P. Linke, J. Makovitzky, Histochemical and topo-optical investigations on tissue-isolated and in vitro amyloid fibrils. *Amyloid*, 2005, 12, 174-183.

[22] J. Hardy, D.J. Selkoe, The amyloid hypothesis of Alzheimer's disease progress and problems on the road to therapeutics. *Science*, 2002, 297, 353-356.

[23] E. Gowing, A.E. Roher, A.S. Woods, R.J. Cotter, M. Chaney, S.P. Little, M.J. Ball, Chemical characterization of Abeta 17-42 peptide, a component of diffuse amyloid deposits of Alzheimer disease. *J. Biol. Chem.* 1994, 269, 10987-10990.

[24] C. Haass, M.G. Schlossmacher, A.Y. Hung, C. Vigo-Pelfrey, A. Mellon, B.L. Ostaszewski, I. Lieberburg, E.H. Koo, D. Schenk, D.B. Teplow, Amyloid beta-peptide is produced by cultured cells during normal metabolism. *Nature*, 1992, 359, 322-325.

[25] T. Iwatsubo, A. Odaka, N. Suzuki, H. Mizusawa, N. Nukina, Y. Ihara, Visualization of A beta 42(43) and A beta 40 in senile plaques with end-specific A beta monoclonals: evidence that an initially deposited species is A beta 42(43). *Neuron.*, 1994, 13, 45-53.

[26] J.P. Blass, Alzheimer's disease. *Dis. Mon.*, 1985, 31, 1-69.

[27] D.M. Walsh, D.M. Hartley, Y.Kusumoto, Y. Fezoui, M.M. Condron, A. Lomakin, G.B. Benedek, D.J. Selkoe, D.B. Teplow, Amyloid beta-protein fibrillogenesis. Structure and biological activity of protofibrillar intermediates. *J. Biol. Chem.*, 1999, 274, 25945-25952.

[28] M. Arimon, I. Diez-Perez, M.J. Kogan, N. Durany, E. Giralt, F. Sanz, X. Fernandez-Busquets, Fine structure study of Abeta1-42 fibrillogenesis with atomic force microscopy. *FASEB J.*, 2005, 19, 1344-1346.

[29] O.S. Makin, E. Atkins, P. Sikorski, J. Johansson, L.C. Serpell, Molecular basis for amyloid fibril formation and stability. *Proc. Natl. Acad. Sci.*, 2005, 102, 315-320.

[30] Y. Fezoui, D.M. Hartley, J.D. Harper, R. Khurana, D.M. Walsh, M.M. Condron, D.J. Selkoe, P.T. Lansbury Jr, A.L.Fink, D.B. Teplow, An improved method of preparing the amyloid beta-protein for fibrillogenesis and neurotoxicity experiments. *Amyloid*, 2000, 7, 166-178.

[31] P.E. Fraser, L.K. Duffy, M.B. O'Malley, J. Nguyen, H. Inouye, D.A. Kirschner, Morphology and antibody recognition of synthetic beta-amyloid peptides. *J. Neurosci. Res.*, 1991, 28, 474-485.

[32] M.A. Westerman, D. Cooper-Blacketer, A. Mariash, L. Kotilinek, T. Kawarabayashi, L.H. Younkin, G.A. Carlson, S.G. Younkin, K.H. Ashe, The relationship between Abeta and memory in the Tg2576 mouse model of Alzheimer's disease. *J. Neurosci.* 2002, 22, 1858-1867.

[33] A.E. Roher, M.O. Chaney, Y.M. Kuo, S.D. Webster, W.B. Stine, L.J. Haverkamp, A.S. Woods, R.J. Cotter, J.M. Tuohy, G.A. Krafft, B.S. Bonnell, M.R. Emmerling, Morphology and toxicity of Abeta-(1-42) dimer derived from neuritic and vascular amyloid deposits of Alzheimer's disease. *J. Biol. Chem.*, 1996, 271, 20631-20635.

[34] Y.M. Kuo, M.R. Emmerling, C. Vigo-Pelfrey, T.C. Kasunic, J.B. Kirkpatrick, G.H. Murdoch, M.J. Ball, A.E. Roher, Water-soluble Abeta (N-40, N-42) oligomers in normal and Alzheimer disease brains. *J. Biol. Chem.*, 1996, 271, 4077-4081.

[35] M.P. Lambert, A.K. Barlow, B.A. Chromy, C. Edwards, R. Freed, M. Liosatos, T.E. Morgan, I. Rozovsky, B. Trommer, K.L. Viola, P. Wals, C. Zhang, C.E. Finch, G.A. Krafft, W.L. Klein, Diffusible, nonfibrillar ligands derived from Abeta1-42 are potent central nervous system neurotoxins. *Proc. Natl. Acad. Sci.*, 1998, 95, 6448-6453.

[36] D.M. Hartley, D.M. Walsh, C.P. Ye, T. Diehl, S. Vasquez, P.M. Vassilev, D.B. Teplow, D.J. Selkoe, Protofibrillar intermediates of amyloid beta-protein induce acute electrophysiological changes and progressive neurotoxicity in cortical neurons. *J. Neurosci.*, 1999, 19, 8876-8884.

[37] J.Y. Lee, J.E. Friedman, I. Angel, A. Kozak, J.Y. Koh, The lipophilic metal chelator DP-109 reduces amyloid pathology in brains of human beta-amyloid precursor protein transgenic mice. *Neurobiol. Aging.*, 2004, 25, 1315-1321.

[38] A. Dedeoglu, K. Cormier, S. Payton, K.A. Tseitlin, J.N. Kremsky, L. Lai, X. Li, R.D. Moir, R.E. Tanzi, A.I. Bush, N.W. Kowall, J.T. Rogers, X. Huang, Preliminary studies of a novel bifunctional metal chelator targeting Alzheimer's amyloidogenesis. *Exp. Gerontol.*, 2004, 39, 1641-1649.

[39] B. Solomon, R. Koppel, D. Frankel, E. Hanan-Aharon, Disaggregation of Alzheimer beta-amyloid by site-directed mAb. *Proc. Natl. Acad. Sci. USA*, 1997, 94, 4109-4112.

[40] S. Gilman, M. Koller, R.S. Black, L. Jenkins, S.G. Griffith, N.C. Fox, L. Eisner, L. Kirby, M.B. Rovira, F. Forette, J.M. Orgogozo, Clinical effects of Abeta immunization (AN1792) in patients with AD in an interrupted trial. *Neurology*, 2005, 64, 1553-1562.

[41] F. Bard, C. Cannon, R. Barbour, R.L. Burke, D. Games, H. Grajeda, T. Guido, K. Hu, J. Huang, K. Johnson-Wood, K. Khan, D. Kholodenko, M. Lee, I. Lieberburg, R. Motter, M. Nguyen, F. Soriano, N. Vasquez, K. Weiss, B. Welch, P. Seubert, D. Schenk, T. Yednock, Peripherally administered antibodies against amyloid beta-peptide enter the central nervous system and reduce pathology in a mouse model of Alzheimer disease. *Nat. Med.*, 2000, 6, 916-919.

[42] Y. Levites, P. Das, R.W. Price, M.J. Rochette, L.A. Kostura, E.M. McGowan, M.P. Murphy, T.E. Golde, Anti-Abeta42- and anti-Abeta40-specific mAbs attenuate amyloid deposition in an Alzheimer disease mouse model. *J. Clin. Invest.*, 2006, 116, 193-201.

[43] C. Soto, M.S. Kindy, M. Baumann, B. Frangione, Inhibition of Alzheimer's amyloidosis by peptides that prevent beta-sheet conformation. *Biochem. Biophys. Res. Commun.*, 1996, 226, 672-680.

[44] J.F. Poduslo, G.L. Curran, A. Kumar, B. Frangione, C. Soto, Beta-sheet breaker peptide inhibitor of Alzheimer's amyloidogenesis with increased blood-brain barrier permeability and resistance to proteolytic degradation in plasma. *J. Neurobiol.*, 1999, 39, 371-382.

[45] M.A. Findeis, J.-J. Lee, M. Kelley, J. Wakefield, M.H. Zhang, J. Chin, W. Kubasek, M.H. Zhang, S.M. Molineaux, Characterization of cholyl-leu-val-phe-phe-ala-OH as an inhibitor of amyloid beta-peptide polymerization. *Amyloid*, 2001, 8, 231-241.

[46] R.J. Chalifour, R.W. McLaughlin, L. Lavoie, C. Morissette, N. Tremblay, M. Boule, P. Sarazin, D. Stea, D. Lacombe, P. Tremblay, F. Gervais, Stereoselective interactions of peptide inhibitors with the beta-amyloid peptide. *J. Biol. Chem.*, 2003, 278, 34874-34881.

[47] Y. Matsunaga, A. Fujii, A. Awasthi, J. Yokotani, T. Takakura, T. Yamada, Eight-residue Abeta peptides inhibit the aggregation and enzymatic activity of Abeta42. *Regul. Pept.*, 2004, 120, 227-236.

[48] S. Gilead, E. Gazit, Inhibition of amyloid fibril formation by peptide analogues modified with alpha-aminoisobutyric acid. *Angew. Chem. Int. Ed.*, 2004, 43, 4041-4044.

[49] H.A. Lashuel, D.M. Hartley, D. Balakhaneh, A. Aggarwal, S. Teichberg, D.J.E. Callaway, New class of inhibitors of amyloid-beta fibril formation. Implications for the mechanism of pathogenesis in Alzheimer's disease. *J. Biol. Chem.*, 2002, 277, 42881-42890.

[50] F.G. De Felice, M.N.N. Vieira, L.M. Saraiva, J.D. Figueroa-Villar, J. Garcia-Abreu, R. Liu, L. Chang, W.L. Klein, S.T. Ferreira, Targeting the neurotoxic species in Alzheimer's disease: inhibitors of Abeta oligomerization. *FASEB J.*, 2004, 18, 1366-1372.

[51] R. Liu, H. Barkhordarian, S. Emadi, C.B. Park, M.R. Sierks, Trehalose differentially inhibits aggregation and neurotoxicity of beta-amyloid 40 and 42. *Neurobiol. Dis.*, 2005, 20, 74-81.

[52] P. Kapkova, V. Alptuzun, P. Frey, E. Erciyas, U. Holzgrabe, Search for dual function inhibitors for Alzheimer's disease: Synthesis and biological activity of acetylcholinesterase inhibitors of pyridinium-type and their Abeta fibril formation inhibition capacity. *Bioorg. Med. Chem.*, 2005, 472-478.

[53] O. Crescenzi, S. Tomaselli, R. Guerrini, S. Salvadori, A.M. D'Ursi, P.A. Temussi, D. Picone, Solution structure of the Alzheimer amyloid beta-peptide (1-42) in an apolar microenvironment. Similarity with a virus fusion domain. *Eur. J. Biochem.* 2002, 269, 5642-5648.

[54] Y. Kallberg, M. Gustafsson, B. Persson, J. Thyberg, J. Johansson, Prediction of amyloid fibril-forming proteins. *J. Biol. Chem.*, 2001, 276, 12945-12950.

[55] K. Janek, S. Rothemund, K. Gast, M. Beyermann, J. Zipper, H. Fabian, M. Bienert, E. Krause, Study of the conformational transition of A beta(1-42) using D-amino acid replacement analogues. *Biochemistry,* 2001, 40, 5457-5463

[56] N. Sreerama, R.W. Woody, Estimation of protein secondary structure from circular dichroism spectra: comparison of CONTIN, SELCON, and CDSSTR methods with an expanded reference set. *Anal. Biochem.*, 2000, 287, 252-260.

[57] N. Sreerama, R.W. Woody, A self-consistent method for the analysis of protein secondary structure from circular dichroism. *Anal. Biochem.*, 1993, 209, 32-44.

[58] S.W. Provencher, J. Glöckner, Estimation of globular protein secondary structure from circular dichroism. *Biochemistry*, 1981, 20, 33-37.

[59] W. C. Johnson, Analyzing protein circular dichroism spectra for accurate secondary structures. *Proteins: Struct. Funct. Genet.*, 1999, 35, 307-312.

[60] N. Greenfield, G.D. Fasman, Computed circular dichroism spectra for the evaluation of protein conformation. *Biochemistry*, 1969, 8, 4108-4116.

[61] J.D. Morrisett, J.S.K. David, H.J. Pownall, A.M. Gotto Jr., Interaction of an apolipoprotein (apoLP-alanine) with phosphatidylcholine. *Biochemistry*, 1973, 12, 1290-1299.

[62] A.E. Roher, J.D. Lowenson, S. Clarke, A.S. Woods, R.J. Cotter, E. Gowing, M.J. Ball, Beta-Amyloid-(1-42) is a major component of cerebrovascular amyloid deposits: implications for the pathology of Alzheimer disease. *Proc. Natl. Acad. Sci.*, 1993, 90, 10836-10840.

[63] F. Prelli, E. Castano, G.G. Glenner, B. Frangione, Differences between vascular and plaque core amyloid in Alzheimer's disease. *J. Neurochem.* 1988, 51, 648-651.

[64] J. Davis, W.E. Van Nostrand, Enhanced pathologic properties of Dutch-type mutant amyloid beta-protein. *Proc. Natl. Acad. Sci*, 1996, 93, 2996-3000.

[65] C.T. Mant, R.S. Hodges, Analysis of peptides by high-performance liquid chromatography. *Methods Enzymol.,* 1996, 271, 3-50.

[66] C.L. Shen, G.L. Scott, F. Merchant, R.M. Murphy, Light scattering analysis of fibril growth from the amino-terminal fragment beta(1-28) of beta-amyloid peptide. *Biophys. J.*, 1993, 65, 2383-2395.

[67] L.O. Tjernberg, D.J.E. Callaway, A. Tjernberg, S. Hahne, C. Lilliehook, L. Terenius, J. Thyberg, C. Nordstedt, A molecular model of Alzheimer amyloid beta-peptide fibril formation. *J. Chem. Biol.*, 1999, 274, 12619-12625.

[68] O. Crescenzi, S. Tomaselli, R. Guerrini, S. Salvadori, A.M. D'Ursi, P.A. Temussi, D. Picone, Solution structure of the Alzheimer amyloid beta-peptide (1-42) in an apolar microenvironment. Similarity with a virus fusion domain. *Eur. J. Biochem.* 2002, 269, 5642-5648.

[69] A.Paivio, E. Nordling, Y. Kallberg, J. Thyberg, J. Johansson, Stabilization of discordant helices in amyloid fibril-forming proteins. *Prot. Sci.*, 2004, 13, 1251-1259.

[70] M. Calero, M. Gasset, Fourier transform infrared and circular dichroism spectroscopies for amyloid studies. *Methods Mol. Biol.*, 2005, 299, 129-151.

[71] N.J. Greenfield, Analysis of circular dichroism data. *Methods Enzymol.* 2004, 383, 282-288.

[72] N.J. Greenfield, Methods to estimate the conformation of proteins and polypeptides from circular dichroism data. *Anal. Biochem.*, 1996, 235, 1-10.

[73] C.L. Shen, M.C. Fitzgerald, R.M. Murphy, Effect of acid predissolution on fibril size and fibril flexibility of synthetic beta-amyloid peptide. *Biophys. J.*, 1994, 67(3), 1238-1246.

[74] G. Bitan, D.B. Teplow, Preparation of aggregate-free, low molecular weight amyloid-beta for assembly and toxicity assays. *Methods Mol. Biol.*, 2005, 299, 3-9.

[75] C.J. Barrow, A. Yasuda, P.T.M. Kenny, M.G. Zagorski, Solution conformations and aggregational properties of synthetic amyloid beta-peptides of Alzheimer's disease. Analysis of circular dichroism spectra. *J. Mol. Biol.*, 1992, 225, 1075-1093.

Chapter 2: Composition and biological activity of traditional and commercial kava extracts

2.1 LITTERATURE REVIEW

2.1.1 Traditional kava extract

Piper methysticum is a plant from the South Pacific Island commonly named Kava, Kava-Kava, Awa, Ava pepper or Yangona. In the eighteenth-century, European explorers described kava consumption as an important activity of the Pacific Islanders. At that time, the traditional kava beverage was a fundamental part of the religious, political and economical life of the Islanders. Today, kava consumption is no longer reserved to special events and aborigines consume it on a daily basis in their social life and as complementary medicine. Similar to the use of alcohol in the Western Countries, the traditional kava beverage is ingested to increase sociability, feelings of peace and relaxation. Unlike alcohol, kava drinks do not increase the drinkers' aggressiveness and do not decrease their ability to drive or think clearly[76].

The traditional kava beverage is prepared from the rhizomes of *Piper methysticum.* The Islanders prepare this beverage with ground kava roots (1.0-1.5 g) infused in cold water or coconut milk (100 to 150 ml). A series of lactones, named kavalactones, have been identified as the active ingredients of this kava extracts. Many studies have shown that the concentrations of kavalactones vary from one cultivar to another and also with the plant age and environment[77]. More than eighteen kavalactones have been identified in kava extracts. Methysticin (M), dihydromethysticin (DHM), kavain (K), dihydrokavain (DHK), demethoxyyangonin (DMY) and yangonin (Y) are kavalactones found in almost all cultivars and they account for ~96% of the kavalactone content[1]. Structures for these six kavalactones are presented in Figure 31.

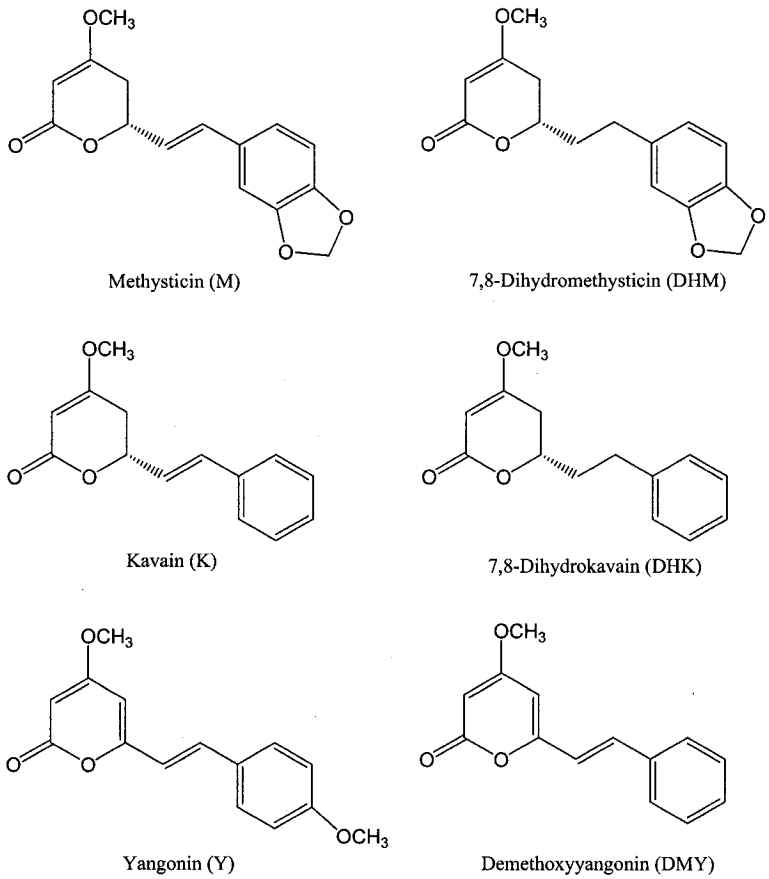

Figure 18 - Structures for the six major kavalactones of kava extracts

Kavalactones are biologically active molecules with important pharmacological properties. For example, 210 mg/day of kavalactones show an effect similar to that of 15 mg/day of oxazepam or 9 mg/day of bromazepam on the Hamilton Anxiety scale which is used to evaluate the efficiency of anxiolytic drugs[78]. Another example is the analgesic effect of DHK and DHM. In fact, 120 mg/kg of either DHK or DHM is equivalent to 200 mg/kg of acetylsalicylic acid[79]. Numerous clinical studies suggest that kavalactones are effective at treating anxiety and nervous conditions[80,81,82,83]. Pre-clinical studies have demonstrated their analgesic, anticonvulsant, psychotropic, local anesthetic, sedative and muscular relaxant activities[1,2,4,84,85,86]. Some physiological properties of the kavalactones might

explain, at least in part, the clinical activities of kavalactones. For example, the psychotropic activity of kavalactones may be explained by their interaction with the GABA-A receptor and/or its inhibition of noradrenaline uptake[7].

Side effects reported after kava ingestion are mild and reversible. At the recommended dose of 40 to 210 mg/day and for a short period of time, 1-24 weeks, side effects reported include nausea, allergic skin reactions and change in liver enzyme concentrations (e.g. increases in alanine aminotransferase and gamma-glutamyl transferase)[87,88,89]. More serious side effects have been reported for heavy kava drinkers. Chronic consumption of kava, sometimes 100 times above the recommended dosage, may lead to hair loss, skin rash, yellowish discoloration of the skin, ulcerous skin, visual difficulties and weight loss [1,10].

In summary, the safety of traditional kava and its efficacy are now widespread. Since 1990, Europeans and North Americans consume the unlicensed commercial kava extract to treat anxiety problems and insomnia[90].

2.1.2 Commercial extracts

The sale of kava supplements, like many herbal remedies, grew exponentially during the 1990's. For example, the American Botanical Council reports that U.S. kava sales were above $30 millions in 2000[91]. At that time, the kava extract was among the top 10 sellers of herbal supplement.

Between 1999 and 2002 more then 82 cases of liver failure were attributed to commercial kava extracts[92,93,94,95,96,97,98,99]. This includes several cases where jaundice and/or hepatitis have led to liver transplant and/or mortality. Two cases have been attributed to depletion of human CYP2D6, the enzyme responsible for the metabolism of kavalactones[100,101,102]. Most other cases involved concomitant ingestion of drugs known for their potential hepatotoxicity, which suggests that herb-drug interactions may be implicated[21]. In 2002, acting in response to theses cases, Germany removed all kava extracts from the market[103]. Today, kava is banned in many countries including Canada, United Kingdom, Australia and all European countries[104]. In the United States, kava extracts are under investigation and consumers are warned of its potential hepatotoxicity[105].

Many hypotheses have been proposed to explain why within two decades several cases of hepatotoxicity were reported for the commercial kava extracts whereas traditional kava has been used safely for many centuries[106,107,108]. Most of these hypotheses point toward the preparation of the commercial extract. One of the concerns lies in the part of the kava plant employed by manufacturers. In order to optimize extraction of kavalactones, some manufacturers use the entire kava plant instead of the rhizome. It is well-documented that the aerial part of kava plant contains toxic alkaloids[109]. Others have suggested that manufacturers raise the amount of kavalactones in their standardized extracts with synthetic ones. By doing so, they add racemic kavalactones to the commercial extract whereas the natural extract contains only one enantiomer[21]. The last difference is the use of organic solvents as opposed to water, which may affect the composition of the extract. Organic solvents utilized in the preparation of commercial extracts include ethanol, methanol, acetone and organic solvent-water mixtures[21,25,27]. Whitton *et al.* observed

slight variations of the kavalactone:glutathione ratio depending on the solvent used for extraction[110]. Qualitative analysis of the composition using thin layer chromatography was reported for the commercial and the traditional kava extracts. The authors conclude that compositions are similar for both extracts although the method is only qualitative and two of the six major kavalactones were not detected[111]. More information about the composition of the kava extracts must be collected in order to determine if some toxic molecules are extracted using organic solvents and to determine if the ratio of kavalactones vary in organic versus aqueous extracts.

As stated above, the majority of hepatotoxic cases reported for the commercial kava extract involve concomitant ingestion of pharmaceuticals, suggesting herb-drug interactions via human cytochrome P450 enzymes (P450s or CYPs).

2.1.3 Cytochrome P450 enzymes (CYPs)

Drug metabolism in mammals is generally divided in two phases. In phase I, a polar group is introduced into the molecule to facilitate its excretion in urine and/or to prepare the molecule for additional metabolism. In phase II metabolism, polar molecules or phase I metabolites are conjugated to endogenous molecules such as glutathione or glucoronic acid to produce soluble metabolites[112].

CYPs are implicated in phase I metabolism. They oxidize more than 90% of the current pharmaceuticals[113]. They do so by catalyzing numerous reactions such as hydroxylations, epoxidations, N-, O- or P-dealkylations, N-, S- or P-oxidations, desulfurations, dehalogenations, nitro and azo reductions[114].

The name P450 originates from the characteristic absorption peak at 450 nm observed when these enzymes are reduced and bound to carbon monoxide[115]. The nomenclature system commonly used for CYPs was proposed in 1987 by Nebert *et al.*[116]. The different isoforms are grouped into a family (Arabic number) if the gene sequences are ≥40% homologous. Families are subsequently divided into subfamilies (letter) if the sequence homology is superior to 55%. The individual isozymes of a subfamily are identified using a second Arabic number[117]. For example, CYP2C9 and CYP2D6 belong to the same CYP family (family 2) but belong to different subfamilies (C and D respectively). In addition, CYP2C9 was the ninth isoform identified in the CYP2C subfamily.

Crystal structures of many human P450 enzymes[118,119,120,121,122,123] and several structure-activity relationships studies provide a plethora of structural information for P450

enzymes. Although, amino acid sequences vary greatly among CYPs, their structural folds and active sites are highly conserved. All CYPs present a common heme-cofactor at their active site (Figure 32). The proximal side of the porphyrin is attached to the enzyme via a cysteine thiolate. In the resting state, the distal side is bound to a water molecule.

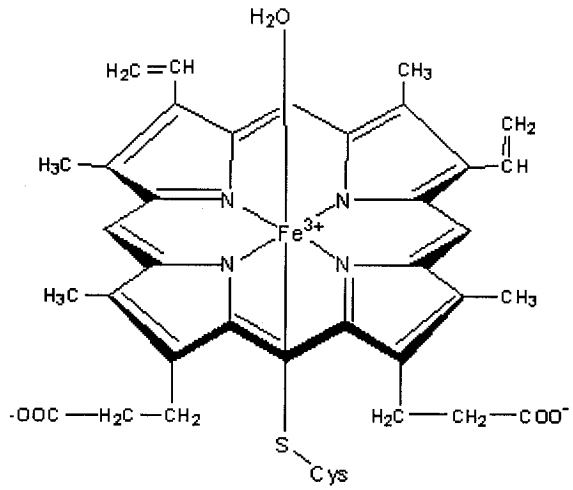

Figure 19 – Heme iron ligation state of the P450 cofactor.

CYPs are believed to share a common mechanism for which some of the mechanistic details remain unclear. The generally recognized steps in the catalytic cycle of CYPs are described in Figure 33[38,40,124]. The cycle is initiated by binding of the substrate (**RH**) to the enzyme which displaces the distal water molecule (step **I.** to **II.**). This is accompanied by a change in the spin state, from a low spin hexacoordinated ferric enzyme to a high spin pentacoordinated ferric enzyme. This leads to a raise in the redox potential of the system. During the second step, one electron is transferred from the redox partners (NADPH and cytochrome P450 reductase) to reduce the ferric porphyrin to ferrous (**III.**). Ferrous heme enzymes have a high affinity for molecular oxygen which leads to the formation of an

oxyferrous complex (**IV.**). The enzyme-bound ferrous heme (**III.**) may alternatively react with carbon monoxide to form a ferrous-CO complex (**IIIa.**) which gives rise to the characteristic absorption at 450 nm and also inhibits CYP activity. Subsequently, the oxyferrous complex (**IV.**) accepts a second electron followed by a proton to form a hydroxyperoxide complex (**V.**). The hydroxyperoxide complex accepts a second proton and releases a water molecule to form an oxoferryl complex (**VI.**). This oxoferryl complex abstracts a hydrogen atom from the substrate to generate a radical substrate (**R·**) and a one-electron reduced ferryl species (**VII.**). Then, the radical substrate (**R·**) recombines with the hydroxyl radical to yield the enzyme-product complex (**VIII.**). Finally, the enzyme releases the product (**ROH**) and binds a water molecule to regenerate the resting low spin hexacoordinated ferric enzyme.

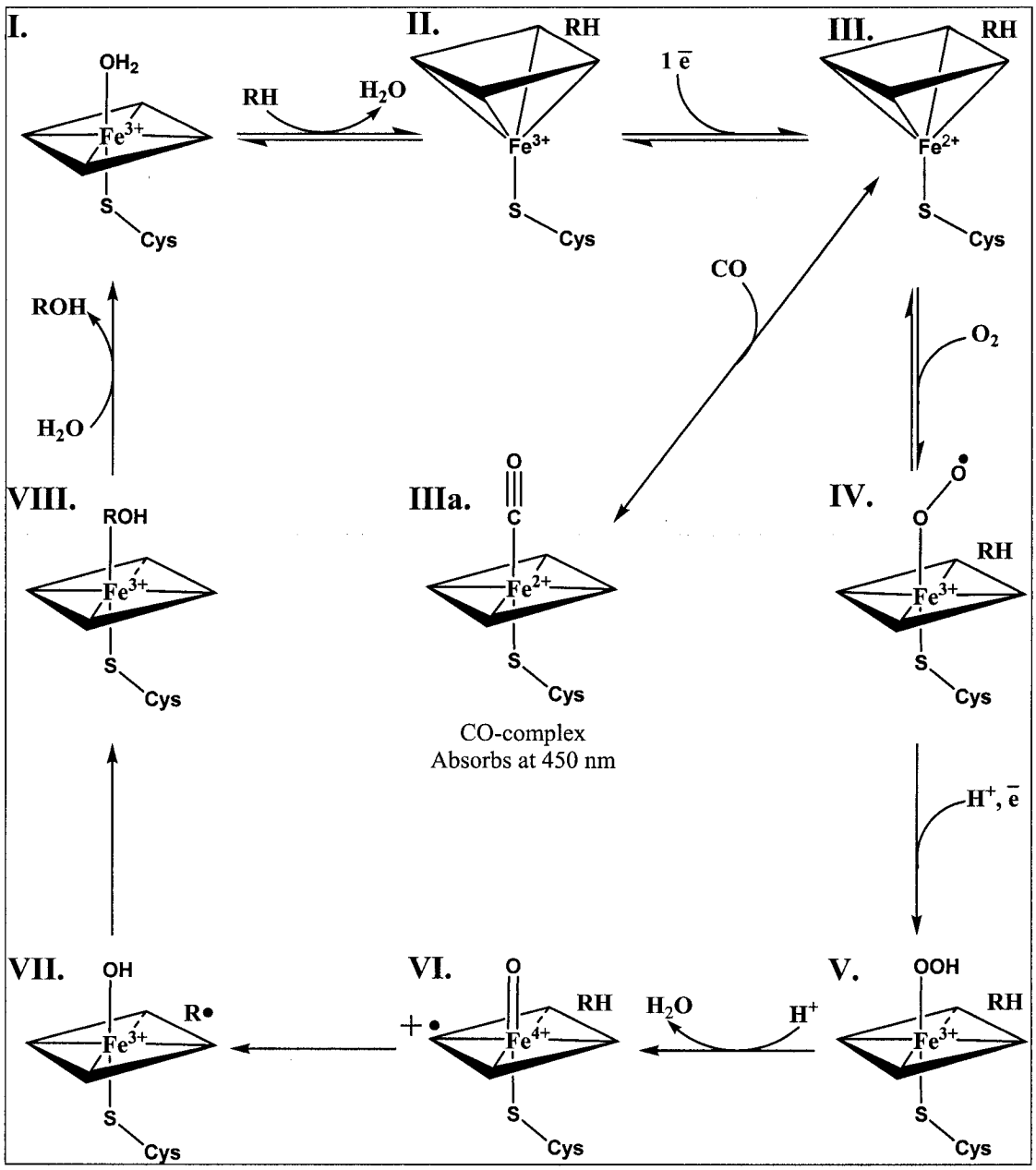

Figure 20 - Generally accepted catalytic mechanism of CYPs. The square symbol represents the heme cofactor bound to the enzyme via a cysteine residue. The substrate is abbreviated by RH.

Since, NADPH and cytochrome P450 reductase (CPR) are required to reduce P450s, the overall hydroxylation reaction by these enzymes can be summarized by Equation 4.

$$RH + O_2 + P450 + NADPH + H^+ + CPR \rightarrow ROH + H_2O + NADP^+ + P450 + CPR \quad \textbf{Eq 4}$$

2.1.4 Drug-drug interactions

The modulation of P450 activity has been implicated in many adverse drug reactions. Their activation or suppression may have dramatic effects on the metabolism of drugs. For this reason, pharmaceutical drugs are required to undergo extensive pharmacological characterization, including the quantification of CYP interactions, before approval by governmental agencies. Sales of herbal remedies and dietary supplements are authorized without pharmacokinetic evaluations. This lack of regulation sometimes leads to herb-drug interactions. St-John's Wort, Gingko Biloba, Echinacea, garlic and grapefruit juice are examples of "natural" modulators of P450 activity interfering with the metabolism of prescribed drugs[125,126].

The modulation of P450 activity by drugs/herbs is often established by *in vitro* assays with P450 enzyme solutions such as microsomes. The assay consists of the incubation of the enzyme with a substrate, NADPH, CPR and O_2, with or without the molecule under investigation. The enzyme activity is quantified by fluorescence, UV/Vis spectroscopy or HPLC to determine the effect of the molecule of interest. Drug/herb interactions are to be expected when a given molecule inhibits or induces human P450 enzyme activity.

Kavalactones and commercial kava extracts have been reported to inhibit P450 activity[127,128,129]. Before our studies, the effect of traditional kava extract on the activity of

P450s had never been investigated. The results obtained by Zou *et al.* [53] for the distinct kavalactones are summarized in Table 2. The CYP isoforms tested for the six major kavalactones and the commercial extracts were CYP1A2, CYP2C9, CYP2C19, CYP2D6 and CYP3A4. The IC_{50} values reported were in the micromolar range which corresponds to significant P450 inhibition.

Table 11 - IC_{50}s reported for the six major kavalactones on the activitiy of five human P450 isoforms, adapted from Zou *et al.*[53]

CYP IC_{50} (→) Kavalactones (↓)	1A2 (μM)	2C9 (μM)	2C19 (μM)	2D6 (μM)	3A4 (μM)
Methysticin	12.53	16.39	0.93	153.2	10.20
Dihydromethysticin	14.8	13.35	0.43	37.03	11.4
Kavain	44.66	128.3	4.86	N.E.	N.E.
Dihydrokavain	N.E.	130.9	10.05	N.E.	N.E.
Yangonin	19.87	N.E.	22.57	N.E.	N.E.
Demethoxyyangonin	1.70	50.12	0.51	N.E.	N.E.

N.E. = No effect reported at the highest concentration tested.

The results reported by Matthew et *al.*[52] are similar to the ones described above. However, additional experiments were performed to demonstrate that methysticin and dihydromethysticin form a metabolite intermediate complex with the enzyme which leads to mechanism-based inhibition.

In summary, commercial and traditional kava extracts seem to present different toxicity profiles. Before our studies, qualitative and quantitative analyses of organic and aqueous kava extracts had not been carried simultaneously and comparisons were difficult. Moreover, although the inhibition of human P450s by individual kavalactones and commercial kava extracts had been reported, similar studies had not been reported for the traditional kava extract.

The aim of this second project was to extract kava roots with water, ethanol, acetone and methanol to mimic the traditional (aqueous) and the commercials (organic) extracts respectively. The resulting extracts were next analyzed to identify and quantify the kavalactone constituents. Variations in the relative amounts of the kavalactones were also evaluated. Finally, the different extracts were tested, using a fluorescence-based assay, to determine inhibition of P450 enzyme activity. The following manuscript was published under the reference: C.S. Côté, C. Kor, J. Cohen, K. Auclair, Composition and biological activity of traditional and commercial kava extracts. Biochem. Biophys. Res. Comm., 2004, 322, 147-152.

Composition and biological activity of traditional and commercial kava extracts

Cynthia S. Côté, Christine Kor, Jon Cohen, Karine Auclair*

Department of Chemistry, McGill University, 801 Sherbrooke Street West, Montréal, Québec, Canada H3A 2K6, karine.auclair@mcgill.ca

* Corresponding author. Department of Chemistry, McGill University, 801 Sherbrooke Street West, Montréal, Québec, Canada H3A 2K6; karine.auclair@mcgill.ca; Fax: 514-398-3797 contribution of the co-authors

2.2 ABSTRACT

For centuries the South Pacific Islanders have consumed kava (*Piper methysticum*) as a ceremonial intoxicating beverage. More recently, caplets of kava extracts have been commercialized for their anxiolytic and antidepressant activity. Several cases of hepatotoxicity have been reported following consumption of the commercial preparation whereas no serious health effects had been documented for the traditional beverage. A detailed comparison of commercial kava extracts (prepared in acetone, ethanol or methanol) and traditional kava (aqueous) reveal significant differences in the ratio of the major kavalactones. To show that these variations could lead to differences in biological activity, the extracts were compared for their inhibition of the major drug metabolizing P450 enzymes. In all cases (CYP3A4, CYP1A2, CYP2C9 and CYP2C19), the inhibition was more pronounced for the commercial preparation. Our results suggest that the variations in health effects reported for the kava extracts may result from the different preparation protocols used.

Keywords: Kava; piper methysticum; kavalactone; methysticin; kavain; yangonin; P450; CYP; inhibition; inhibit

2.3 INTRODUCTION

Extracts of *Piper methysticum*, or kava, have been consumed in the South Pacific Islands for centuries without any reported serious side effects[1,25]. The traditional extract is an infusion of ground kava roots (1.0-1.5g) in cold water (100-150 ml) used for its psychotropic and hypnotic properties[10]. The consumption of kava has now spread to the Western world where the traditional kava root infusion has been replaced by commercially available caplets. Sixteen different kavalactones have been identified as the active principles of this extract. Methysticin, dihydromethysticin, kavain, dihydrokavain, demethoxyyangonin and yangonin are the major ones and account for 96% of the organic extract[2].

Reported beneficial effects of kava at low concentrations include relaxation, euphoria, anticonvulsant properties, neuroprotection, analgesia, and attenuation of menopausal symptoms[1-3,9-11]. After being approved for the treatment of anxiety and nervous disorders in 1990[10], kava was banned from Germany in June 2002 based on the reevaluation of its risk-to-benefit ratio by the German Health authorities[21,35,130]. Kava has since been removed from the market in all of Europe (including UK), Australia and Canada, and a warning has been issued in USA[21,25,55]. Many clinical studies suggest that the kava extract offers an effective alternative for the treatment of anxiety[5-8] and conclude that it is relative safe when used alone at recommended dosage for a short period of time (1-24 weeks)[13,14,131]. On the other hand, 78 cases of hepatotoxicity have been reported following ingestion of commercial kava caplets[18,21-22,27,55,132] but none have been recorded for the traditional extract. In several of these cases, the hepatic failure has required liver transplantation or has been fatal[10,18,21-22,25,27,55,57]. Two cases have been attributed to depletion of human

CYP2D6, the enzyme responsible for kavalactone metabolism[9,25,27]. Most other cases involved concomitant ingestion of drugs known for their potential hepatotoxicity[21] or of other pharmaceuticals, which suggests that herb-drug interactions may be implicated.

P450 inhibition or induction is an important factor leading to drug interactions. The inhibition of human P450 isoforms CYP1A2, CYP2C9, CYP2C19, CYP2D6, CYP3A4 and CYP4A9/11 (from either microsomes or human hepatocytes) by individual kavalactones, by commercial kava caplets, and by an ethanolic kava root extract have been reported[52-54]. This family of enzymes is important for the degradation of toxins and pharmaceuticals, and for the biosynthesis of steroids and prostaglandins. P450s are most abundant in the liver where a few isoforms, namely CYP1A2, CYP2C9, CYP2C19, CYP2D6 and CYP3A4, account for 80% of the total hepatic metabolism[38]. One of the most promiscuous human isoforms, CYP3A4, is involved in the phase I metabolism of more than 50% of the current pharmaceuticals. It is also the major P450 in the small intestine, whereas CYP2D6, the enzyme responsible for kavalactones metabolism[9,25,27] is the main P450 in the brain[38].

Although the hepatoxicity of kava is still debated[27], multiple hypotheses have been proposed to explain the difference in toxicity between the commercial caplets and the traditional kava extracts. Commercially available kava caplets are usually prepared by ethanolic or acetonic extraction of the full plant[25,36]. Since kava has traditionally been consumed as a water infusion of the root, it has been suggested that the use of organic solvents may extract more toxic components from the kava plant[25]. The use of the aerial part of the plant by the producers of kava caplets is also suspected to lead to toxicity of the

extract. Indeed, the cytotoxic alkaloid pipermethysticin has recently been isolated from this part of the plant[34]. Finally, it has been suggested that the addition of a racemic mixture of synthetic kavain, sometimes added to boost the activity of the commercial extract, may increase the toxicity[21].

Our aim was to compare kava root extracts prepared using water, methanol, ethanol or acetone by analytical methods. The ratio of the major kavalactones of the aqueous extract was found to be different from that of all other extracts and it was envisaged that theses disparities could lead to variations in biological activities. This hypothesis was confirmed by comparing the inhibition of the major drug metabolizing human P450s by the aqueous and organic extracts.

2.4 MATERIALS AND METHODS

2.4.1 Chemicals and Enzymes

Human liver CYP1A2 supersomes containing P450 reductase were purchased from BD Gentest (Woburn. MA). Human liver CYP3A4, CYP2D6, CYP2C19 and CYP2C9 microsomes, which included P450 reductase and cytochrome b_5, were also obtained from BD Gentest. The substrates 7-benzyloxy-4-trifluoromethylcoumarin (BFC), 7-methoxy-4-trifluorocoumarin (MFC) and 3-[2-(*N*,*N*-diethyl-*N*-methylamino)ethyl]-7-methoxy-4-methylcoumarin (AMMC), as well as the fluorescent products 7-hydroxy-4-trifluoromethylcoumarin (HFC) and 3-[2-*N*,*N*-diethyl-*N*-methylamino)ethyl]-7-hydroxy-4-methylcoumarin (AHMC) were also purchased from BD Gentest.

The kava roots (Moi variety) were generously provided by Dr. Will McClatchey from Hawaii University (occasionally via Jonathan Yee, a kava farmer in Hawaii). The kavalactone standards methysticin (M), dihydromethysticin (DHM), kavain (K), dihydrokavain (DHK), demethoxyyangonin (DMY) and yangonin (Y) were purchased from ChromaDex (Santa Ana, CA). Kava caplets (150 mg per caplet each containing 45 mg of kavalactones) were from Nature's Resource (Mission Hills, CA). All other reagents were obtained from Sigma-Aldrich (St. Louis, MO). Solvents used were HPLC grade, except acetone which was ACS grade. All the measurements described below were done in duplicate.

2.4.2 Instruments

Kinetic assays were performed in black Costar 96-well microplates. Fluorescence of the products was monitored using a GEMINI XS model microplate reader (Molecular Devices Corp., Sunnyvale, CA). NADPH consumption UV assays were carried out using a Spectra Max 190 model microplate reader (Molecular Devices Corp.). Analytical HPLC analyses were performed on an Agilent 1100 modular system equipped with an autosampler, a quaternary pump system, a photodiode array detector, a fluorescence detector, a thermostatted column compartment and a ChemStation (for LC 3D A.09.03) data system.

2.4.3 Extracts preparation

The kava roots (repeated with two different batches of kava Moi variety, one of the most popular varieties) were dried at 37°C for 48 hours and ground in a coffee grinder. For the preparation of organic kava root extracts, the organic solvent (75 ml of methanol, acetone or ethanol) was added to ground kava root (1 g) and the heterogeneous mixture was shaken at 250 rpm and 40°C for 90 min. The mixture was then filtered to remove the root, the solvent was evaporated *in vacuo* and the residues were each reconstituted in methanol (10 ml). The aqueous kava root extract was generated from ground kava root (1 g) stirred in water (125 ml) at room temperature for 10 min. The mixture was subsequently filtered and lyophilized. The solid was reconstituted in methanol (20 ml). The commercial caplet extract was prepared using the powder from 4 Nature's Resource kava caplets mixed in methanol (75 ml) and shaken at 250 rpm and 40°C for 90 min. The insoluble material was filtered off and the solvent was evaporated *in vacuo*. The residue was reconstituted in methanol (10 ml).

2.4.4 HPLC and LC-MS separation

Separation and quantification of the kavalactones were achieved by HPLC using a modification of the procedure reported by Shao *et al.*[133]. The column used was a 250 x 4.6 mm SYNERGI 4μ Hydro-RP 80Å (Phenomenex, Torrance, CA, USA). Isocratic elution with water:acetonitrile:methanol (52:23:25) was used at a flow rate of 1 ml/min. The absorption spectra were recorded from 200 to 400 nm. Quantification was accomplished at 240 nm for methysticin, dihydromethysticin, kavain and dihydrokavain and at 350 nm for demethoxyyangonin and yangonin. The column was thermostatted at 40°C. Confirmation of the identification of the different kavalactones was achieved by LC-MS and with the use of authentic samples. LC-MS analysis was performed on a Spectra System P4000 (Spectro Separation Products) equipped with a UV 2000 detector and a Finnigan LCQ DUO (ion trap) mass detector setup in Atmospheric Pressure Chemical Ionization (APCI) negative mode, controlled by the X caliber software version 1.2. The elution method was the same as described above.

2.4.5 Stock solutions used for enzyme activity and inhibition studies by fluorescence-based assays

The P450 liver microsomes were diluted in 100 mM (CYP3A4, CYP1A2 and CYP2D6) or 25 mM (CYP2C19 and CYP2C9) potassium phosphate buffer at pH 7.4 to a final concentration of 0.1 μM. The stock solution of BFC (5.5 μM, substrate for CYP3A4 and CYP2C19) was prepared from an aqueous dilution of a 300 μM solution in acetonitrile. The CYP2D6 substrate AMMC was first dissolved in acetonitrile (1 mM) and then diluted in water to 15 μM. MFC, the substrate used with CYP2C9, was similarly prepared by

aqueous dilution to 165μM of a 1 mM solution in acetonitrile. Finally, the stock solution of the CYP1A2 substrate ethoxyresorufin (ER) was prepared by aqueous dilution to 5.5 μM from a 1 mM stock solution in acetonitrile. Their respective products were dissolved in the same solvent mixtures. The coenzyme NADPH was dissolved to give a final concentration of 25 mM in the same buffer used to dilute the enzyme tested. All aqueous solutions were prepared using water from a Milli-Q purification system (Millipore Corporation, Bedford, Mass).

2.4.6 Stock solutions used for NADPH consumption assays

The stock solution of quinidine (16.7 mM), the substrate used with CYP3A4, was prepared in aqueous solution. The CYP1A2 substrate, ER, was dissolve (4.2 mM) in chloroform:acetonitrile (15:85). Finally, the stock solution for the CYP2C9 substrate MFC (2.5 mM) was prepared in potassium phosphate buffer (pH 7.4):acetonitrile (50:50). The stock solution of tolbutamide, a CYP2C19 substrate, was prepared in acetonitrile (195 mM).

2.4.7 Enzyme activity assays

The activity of CYP3A4 and CYP2C19 were assayed by monitoring the debenzylation of BFC to HFC. A solution of CYP3A4 (3.3 nM) and BFC (7.5 μM) in 100 mM potassium phosphate at pH 7.4 (total volume 300 μl) was incubated for 5 min at 37°C. CYP2C19 (15 nM) and BFC (2.3 μM) were diluted in 25 mM potassium phosphate at pH 7.4 (total volume 200 μl) and incubated for 5 min at 37°C. The reactions were initiated by the addition of NADPH (830 or 125 μM for CYP3A4 or CYP2C19 respectively) and they

were monitored at 37°C for 20 min. The production of HFC was followed at an excitation wavelength (λ_{ex}) of 410 nm and an emission wavelength (λ_{em}) of 530 nm.

The activity of CYP1A2 was measured by following the production of resorufin from ER. Each incubation mixture (300 µl) contained EDTA (1.5 mM), CYP1A2 (5 nM) and 7-ethoxyresorufin (1 µM) in 100 mM potassium phosphate at pH 7.4. It was incubated for 5 min at 37°C, and following the addition of NADPH (250 µM), the reaction was monitored at λ_{ex} = 530 nm and λ_{em} = 582 nm for 20 min.

The assay used to study the activity of CYP2C9 involved the demethylation of MFC to HFC at 37°C over 30 min. During these experiments λ_{ex} = 410 nm and λ_{em} = 530 nm were used. The reaction mixture (150 µl) contained CYP2C9 (10 nM), MFC (40 µM) and NADPH (750 µM) in 25 mM potassium phosphate buffer at pH 7.4.

2.4.8 Enzyme inhibition assays

Each experiment was carried in duplicate and included a blank (without enzyme), a control of activity as described above, and appropriate control reactions to ensure the absence of inhibition by the trace of solvents used. The concentrations of aqueous kava extract used for inhibition studies were 0.3, 1.4, 2.9, 4.3, 5.8, 8.7, 10.1, 11.6, 14.5, 17.4, 20.3 and 40.6 µg extract/ml for CYP3A4, 0.1, 1.0, 5.0, 10.0, 20.0, 30.0 and 50.0 µg extract/ml for CYP1A2, 0.1, 1.0, 5.0, 10.0, 15.0, 20.0, 30.0, 40.0, 50.0, 60.0, 70.0, 80.0, 90.0, 120.0, 150.0, 170.0 and 200.0 µg extract/ml for CYP2C9, and 0.1, 0.5, 1.0, 2.0, 4.0, 6.0, 8.0, 10.0, 30.0 and 60.0 µg extract/ml for CYP2C19. The concentrations of acetonic

kava extract used were 0.5, 1.0, 2.0, 3.0, 4.0, 5.0, 7.5, 10.0 and 20.0 μg extract/ml for CYP3A4, 0.01, 1.0, 2.0, 3.0, 4.0, 6.0, 8.0, 10.0 and 100.0 μg extract/ml for CYP1A2, 0.1, 0.5, 1.0, 3.0, 5.0, 10.0, 15.0, 20.0, 25.0, 30.0, 50.0, 70.0 and 100.0 μg extract/ml for CYP2C9, and 0.1, 0.3, 0.5, 0.7, 1.0, 2.0, 3.0, 5.0, 10.0 and 20.0 μg extract/ml for CYP2C19. Finally, the concentrations of commercial kava caplet extract used were 0.3, 0.7, 1.3, 2.6, 5.2 and 10.4 μg extract/ml for CYP3A4, 0.01, 1.0, 2.0, 3.0, 4.0, 6.0, 8.0, 10.0 and 100.0 μg extract/ml for CYP1A2, 0.1, 1.0, 3.0, 5.0, 7.0, 10.0, 25.0 and 50.0 μg extract/ml for CYP2C9, and 0.1, 0.5, 1.0, 1.5, 3.0, 5.0, 10.0, 25.0, 50.0 μg extract/ml for CYP2C19. IC_{50} values were calculated from dose-response curves using GraphPad Prism 4.0. Possible interference with our assays (native fluorescence and/or quenching) from the different components of the kava extracts were verified by HPLC and UV and found not to be significant. No corrections were required on the calibration curves of the fluorescent products.

2.4.9 NADPH consumption assays

To each enzyme (50 nM CYP3A4, CYP2C9, CYP1A2 or CYP2C19) in potassium phosphate buffer at pH 7.4, the desired kava extract (2.5 or 25 μg/ml for the acetone extract and 5 or 50 μg/ml for the other ones), the corresponding substrate (275 μM of quinidine for CYP3A4, 85 μM of MFC for CYP2C9, 1.3 mM tolbutamide for CYP2C19 or 140 μM ER for CYP1A2) and NADPH (830 μM) were added. Control experiments were carried out without inhibitor and without NADPH, separately. The consumption of NADPH was monitored at 37°C for 20 min by fluorescence for CYP2C9 (λ_{ex} = 380 nm, λ_{em} = 420 nm), CYP2C19 (λ_{ex} = 340 nm, λ_{em} = 445 nm) and CYP1A2 (λ_{ex} = 360 nm, λ_{em} = 455 nm) and by absorbance for CYP 3A4 (360 nm).

2.5 RESULTS AND DISCUSSION

Two different batches of kava root (Moi variety, one of the most popular) were ground and extracted separately in water to reproduce the preparation of traditional kava, and in acetone, in ethanol and in methanol to mimic commercial extracts. Commercial kava caplets were also studied to validate our results with the kava root. Identification and quantification of the constituents of each extract was achieved by LC-MS and HPLC (Figure 34). The chromatograms show that the same kavalactones are found in all of the extracts whereas highly polar constituents are present in negligible amounts in the organic extracts and in the caplets (data not shown). The *ratio* of the six major kavalactones however, is significantly different for the aqueous extract (note in particular the very low concentration of yangonin) compared to the organic extracts (acetone, ethanol and methanol) which are almost identical to one another (Figure 35). The commercial kava caplets also displayed a comparable pattern of kavalactones except for kavain and dihydrokavain. The higher proportion of kavain and dihydrokavain detected in the caplets may be explained by a different variety of kava used by the manufacturer, by the standardization of the extract or by the intentional addition of racemic material to increase the biological activity[21]. Calculation of the total amount of kavalactones per mg of extract reveals that the aqueous kava root extract contains the lowest proportion of kavalactones of all the root extracts, as expected from the reported low water solubility of kavalactones (Table 3).

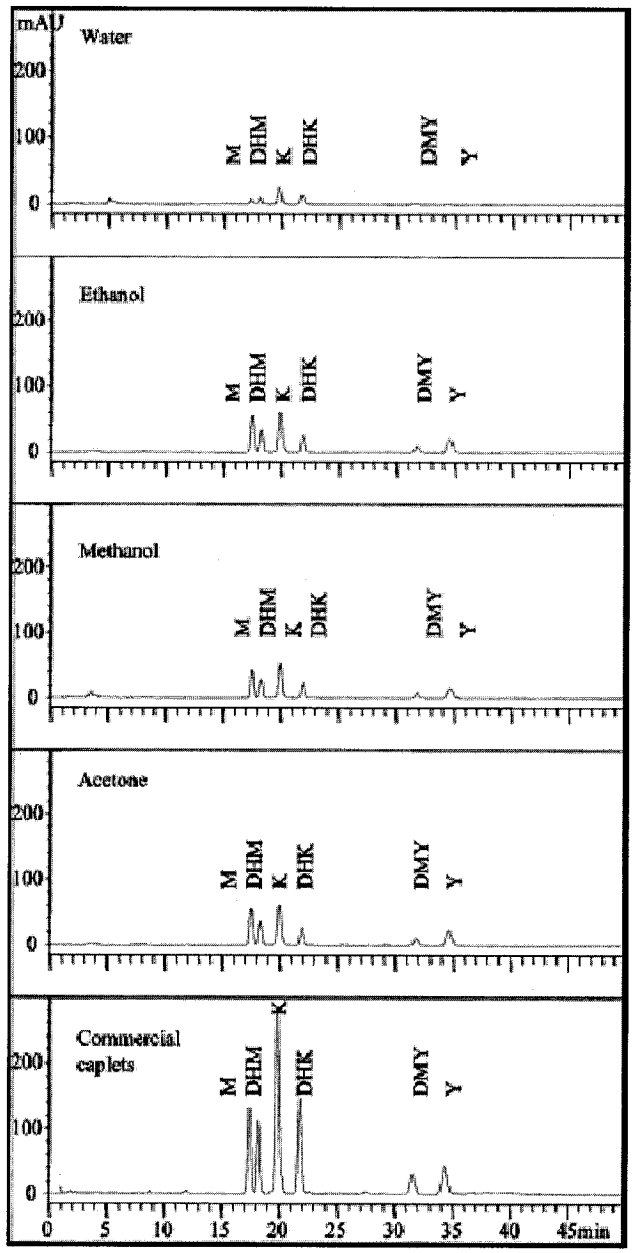

Figure 21 - HPLC chromatograms of the kava root extracts and the commercial kava caplets showing the separation of the six major kavalactones: methysticin (M), dihydromethysticin (DHM), kavain (K), dihydrokavain (DHK), demethoxyyangonin (DMY), and yangonin (Y).

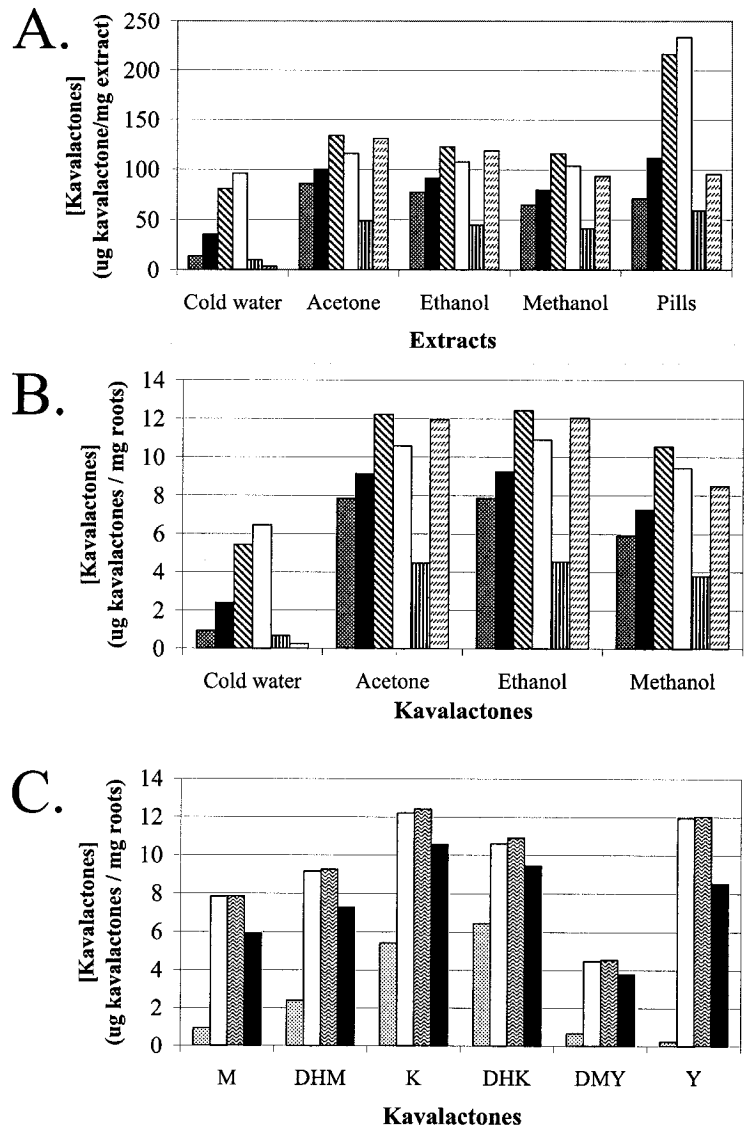

Figure 22 - A) Comparison of the amount of methysticin (▩), dihydromethysticin (■), kavain (▨), dihydrokavain (□), demethoxyyangonin (▥), and yangonin (▨) quantified in kava root extracts and in commercial kava caplets. B) Comparison of the amount of methysticin (▩), dihydromethysticin (■), kavain (▨), dihydrokavain (□), demethoxyyangonin (▥), and yangonin (▨) present in the kava root extract adjusted for the mass of kava root used. C) Same data as B but the histograms are ordered to facilitate comparison of the amount of each kavalactone in the extracts prepared using water (▩), acetone (□), ethanol (▨), or methanol (■). The abbreviations M, DHM, K, DHK, DMY and Y are used for methysticin, dihydromethysticin, kavain, dihydrokavain, demethoxyyangonin and yangonin respectively.

Table 12 - Total amount of kavalactones (KL) in kava root extracts prepared from different solvents and in commercial caplets.

Water	Acetone	Ethanol	Methanol	Caplets
(μg KL/mg extract)	(μg KL/mg extract)	(μg KL/mg extract)	(μg KL/mg extract)	(μg KL/mg extract)
240	616	562	500	788

Differences in the ratio of kavalactones imply possible variations in biological activity. Inhibition of human P450 enzymes is an important pharmacological criterion since it is a primary cause of drug interactions and has been suggested as one possible source of kava hepatotoxicity. Fluorescence-based assays are commonly used to monitor the *in vitro* activity of P450 enzymes however they only allow the detection of the fluorescent product. When another molecule is added, a decrease in formation of the fluorescent product can result from fluorescence quenching, from its competing transformation by the enzyme, or from inhibition of the enzyme by this molecule. NADPH consumption assays were performed to eliminate the possibility that kava extracts be substrates of P450 enzymes as opposed to inhibitors. This assay strongly suggested that the extracts tested all inhibited CYP3A4, CYP2C9 and CYP2C19. In the absence of substrate and in the presence of kava extract, a modest NADPH consumption was detected for CYP1A2, revealing that the extract is transformed by this enzyme but considerably more slowly than 7-ethoxyresorufin. CYP1A2 inhibition was confirmed by a dramatic decrease in NADPH consumption in the presence of both the substrate and the kava extracts. Because of their higher sensitivity, fluorescence-based assays were used for detailed kinetic studies. Control experiments were carried out to validate the methodology (see experimental section). Since

the acetonic, ethanolic and methanolic kava root extracts presented similar concentrations and ratio of kavalactones (Figure 35), P450 inhibition was only tested with the acetonic extract, the aqueous extract and the commercial kava caplets. The results (Table 4) revealed significant inhibition in all cases (here μg/ml ~ μM) yet consistently less inhibition was observed with the aqueous extract. This was expected since kavalactones are known to inhibit P450s[53] and the aqueous extract contains less kavalactones per milligram of extract (Table 3).

Table 13 - Inhibition of human P450 by different kava root extracts and by commercial caplets expressed in μg of extract per ml.

P450 isoform	**IC_{50} waters extract** (μg extract /ml)	**IC_{50} acetone extract** (μg extract /ml)	**IC_{50} caplet** (μg extract /ml)
3A4	7.8 ± 1.3	2.2 ± 0.3	5.9 ± 0.9
1A2	18.4 ± 8.9	4.0 ± 0.6	2.7 ± 0.9
2C9	40.5 ± 13.1	24.8 ± 2.9	5.1 ± 1.8
2C19	3.8 ± 0.3	2.0 ± 0.2	1.8 ± 0.2

Moreover, these results suggest that "non-kavalactones" components present in the aqueous extract don't inhibit P450s significantly. When calculated from the amount of extract, lower inhibition is observed for the aqueous extract with all the enzymes tested. On the other hand, when the IC_{50} is expressed per microgram of kavalactone present in each extract (Table 5), no significant differences are apparent except for CYP2C9. Again, this was expected from the known P450 inhibition by kavalactones[53]. The IC_{50} for the

inhibition of CYP2C9 by the acetonic extract (15.3 µg/ml) is higher than that for the caplet (4.0 µg/ml) and the aqueous extract (9.7 µg ml). Those results may be explained by the increasing amount of yangonin in the different extracts (aqueous < caplet < acetone). Yangonin has been reported by Zou and al.[54] to have no effect on the activity of CYP2C9 and this may explain the lower inhibition by the acetone extract which contained the higher proportion of this kavalactone.

Table 14 - Inhibition of human P450 by different kava root extracts and by commercial caplets expressed in µg of kavalactones per ml.

P450 isoform	**Water extract** (µg kavalactones /ml)	**Acetone extract** (µg kavalactones /ml)	**Caplets** (µg kavalactones /ml)
3A4	1.9 ± 0.3	1.4 ± 0.2	4.6 ± 0.7
1A2	4.4 ± 2.1	2.5 ± 0.4	2.1 ± 0.7
2C9	9.7 ± 3.1	15.3 ± 1.8	4.0 ± 1.4
2C19	0.9 ± 0.1	1.2 ± 0.1	1.4 ± 0.2

2.6 CONCLUSION

In summary, comparison of the traditional aqueous kava with organic kava extracts and commercial kava caplets revealed differences in the ratio of kavalactones which suggest deviations in biological activity. Indeed, although all of the extracts inhibited human CYP3A4, CYP1A2, CYP2C9 and 2C19 in the low μM range, the aqueous extract was the least potent for all these P450s. Kava is often consumed in combination with other pharmaceuticals including antidepressants such as benzodiazepines which are known to be metabolized by CYP3A4[134,135]. Not surprisingly, harmful interactions have been reported between kava and alprazolam[136]. Our results suggest that other potential drug interactions are possible with kava extracts and warrant more *in vivo* studies. Finally, the data presented here indicate that if the hepatotoxicity reported for the commercial caplet is the result of P450 inhibition, the traditional extract should also be hepatotoxic at higher doses.

2.7 ACKNOWLEDGEMENTS

The authors are grateful to Dr. Will McClatchey from Hawaii University and to Jonathan Yee, a kava farmer in Hawaii, for the kava root donations. The authors also wish to thank the Natural Science and Engineering Research Council of Canada, the Fond Quebecois pour la Recherche sur la Nature et les Technologies, and McGill University for providing the funding to carry this research. C. S. Cote was also supported by a scholarship award from the Chemical Biology Strategic Training Initiative of the Canadian Institute of Health Research.

2.8 REFERENCES

[76] V. Lebot, M. Merlin and L. Lindstrom, Kava: the Pacific Drug. Yale University Press, New Haven, 1992.

[77] A.R Clough, C.B. Burns, N. Mununggurr, Kava in Arnhem Land: a review of consumption and its social correlates. *Drug Alcohol Rev.* 2000, 19, 319-328.

[78] V. Schulz, R. Hänsel, V. Tyler, Rational phytotherapy, A physician's guide to herbal medicine. 4th Ed. Springer, Germany (2001).

[79] Y.N. Singh, N.N Singh, Therapeutic potential of kava in the treatment of anxiety disorders. *CNS Drugs*, 2002, 16, 731-743.

[80] J.S. Cauffield, H.J. Forbes, Dietary supplements used in the treatment of depression, anxiety, and sleep disorders. *Lippincotts Prim. Care Pract.*, 1999, 3, 290–304.

[81] E. Ernst, The risk-benefit profile of commonly used herbal therapies: Ginkgo, St. John's Wort, Ginseng, Echinacea, Saw Palmetto and Kava. *Ann. Intern. Med.*, 2002, 136, 42–53.

[82] M.H. Pittler, E. Ernst, Kava extract for treating anxiety. *Cochrane Database Syst. Rev.*, 2004, 2, CD003383.

[83] F.P. Geier, T. Konstantinowicz, Kava treatment in patients with anxiety. *Phytother. Res.* 2004, 18, 297–300.

[84] S.S. Baum, R. Hill, H. Rommelspacher, Effect of kava extract and individual kavapyrones on neurotransmitter levels in the nucleus accumbens of rats. *Prog. Neuro-psychopharmacol. Biol. Physchiat.*, 1998, 22, 1105–1120.

[85] A.R. Bilia, S. Gallori and F.F. Vincieri, Kava–kava and anxiety: growing knowledge about the efficacy and safety. *Life Sci.*, 2002, 70, 2581–2597.

[86] P.A. Whitton, A. Lau, A. Salisbury, J. Whitehouse, C.S. Evans, Kava lactones and the kava-kava controversy. *Phytochem.*, 2003, 64, 673–679.

[87] Y.N. Singh, A.K. Devkota, Aqueous kava extracts do not affect liver function tests in rats. *Planta Med.*2003, 69, 496-499.

[88] A.R. Clough, R.S. Bailie, B. Currie, Liver function test abnormalities in users of aqueous kava extracts. *J. Toxicol. Clin. Toxicol.*, 2003, 41, 821-829.

[89]. S. Russmann, Y. Barguil, P. Cabalion, M. Kritsanida, D. Duhet, B.H. Lauterburg, Hepatic injury due to traditional aqueous extracts of kava root in New Caledonia. *Euro. J. Gastroenterol, Hepatol.*, 2003, 15, 1033-1035.

[90] F. Capasso, T.S. Gaginella, G. Grandolini, A.A. Izzo, Phytotherapy: A quick reference to herbal medicine. Springer-Verlag, Berlin, Heidelberg, 2003.

[91] American Botanical Council Announces New Safety Information on Kava. 2001, December 20 [http://www.herbalgram.org/default.asp?c=122001press].

[92] S. Russmann, B.H. Lauterburg, A. Helbing, Kava hepatotoxicity. *Ann. Intern. Med.*, 2001, 135, 68-69.

[93] M. Escher, J. Desmeules, E. Giostra, G. Mentha, Hepatitis associated with Kava, a herbal remedy for anxiety. *Brit. Med. J.* 2001, 322, 139.

[94] J.V. Campo, J. McNabb, J.M. Perel, G.V. Mazariegos, S.L. Hasegawa, J. Reyes, Kava-induced fulminant hepatic failure. *J. Am. Child Adolesc. Psychiatry*, 2002, 41, 631-632.

[95] Centers for Disease Control and Prevention (CDC), Hepatic toxicity possibly associated with kava-containing products--United States, Germany, and Switzerland, 1999-2002, *MMWR Morb Mortal Wkly. Rep.*, 2002, 51, 1065-1067.

[96] A. Denham, M. McIntyre, J. Whitehouse, Kava-the unfolding story: report on a work-in-progress. *J. Altern. Complement. Med.*, 2002, 8, 237–263.

[97] P.J. Gow, N.J. Connelly, R.L. Hill, P. Crowley, P.W. Angus, Fatal fulminant hepatic failure induced by natural therapy containing kava. *Med. J. Aust.*, 2003, 178, 442-443.

[98] R.B. Brauer, M. Strangl, J.R. Stewart, R. Pfab, K. Becker, Acute liver failure after administration of the herbal tranquilizer kava-kava (*Piper methysticum*). *J. Clin. Psychiatry*, 2003, 64, 216-218.

[99] F.Stickel, H.-M. Baumüller, K. Seitz, D. Vasilakis, G. Seitz, H.K. Seitz, D. Schuppan, Hepatitis induced by kava (*Piper methysticum rhizoma*). *J. Hepatol.*, 2003, 39, 62-67.

[100] R.F.W. Moulds, J. Malani, Kava: herbal panacea or liver poison? *Med. J. Aust.*, 2003, 178, 451–453.

[101] R. Teschke, Kava, kavapyrones and toxic liver injury. *Z. Gastroenterol.*, 2003, 41, 395-404.

[102] J. Anke, I. Ramzan, Kava hepatotoxicity: are we any closer to the truth? *Planta Med.*, 2004, 70, 193–196.

[103] www.bfarm.de/de/Presse/ mitteil_2002/index.php?more=0210.php.

[104] http://www.hc-sc.gc.ca/ahc-asc/media/advisories-avis/2002/2002_56_e.html

[105] http://www.cfsan.fda.gov/~dms/addskava.html

[106] R. Bauer, B. Kopp, A. Nahrstedt, Relevant hepatotoxic effect of kava still need to be proven. *Planta Med.*, 2003, 69, 971-972.

[107] R. Teschke, W. Gaus, D. Loew, Kava extracts: safety and risks including rare hetatotoxicity. *Phytomedecine*, 2003, 10, 440-446.

[108] S.Y. Mills, B. Steinhoff, Kava-kava: a lesson for the phytomedicine community. *Phytomedicine*, 2003, 10, 261-262.

[109] K. Dragull, W.Y. Yoshida and C.-S. Tang, Piperidine alkaloids from *Piper methysticum. Phytochemistry*, 2003, 63, 193–198.

[110] P.A. Witthon, Are kavalactones the hepatotoxic principle of kava extracts? The pitfalls of the glutathione theory. *J. Altern. Complement. Med*, 2003, 9, 183–188.

[111] D. Loew, G. Franz, Quality aspects of traditional and industrial Kava-extracts. *Phytomed.*, 2003, 10, 610–612.

[112] R.L. Rose, E. Hodgson, A textbook of modern toxicology, Third Edition, John Wiley & Sons, 2004, pp 584.

[113] P.R. Ortiz de Montellano, Cytochrome P450 : Structure, Mechanism, and Biochemistry. 3rd Ed. Kluwer Academic/Plenum Publishers, New York, 2005. pp 689.

[114] F.P. Guengerich, Common and uncommon cytochrome P450 reactions related to metabolism and chemical toxicity. *Chem. Res. Toxicol.* 2001,14, 611-650.

[115] L.C. Zoller, J. Weisz, Identification of cytochrome P-450, and its distribution in the membrana granulosa of the preovulatory follicle, using quantitative cytochemistry. *Endocrinology*, 1978, 103, 310-313.

[116] D.W. Nebert, M.Adesnik, M.J. Coon, R.W. Estabrook, F.J. Gonzalez, F. Guengerich, I.C. Gunsalus, E.F. Johnson, B. Kemper, W. Levin, I.R. Phillips, R. Sato, M.R.Waterman, The P450 gene superfamily: recommended nomenclature. *DNA,* 1987, 6, 1-11.

[117] D.W. Nebert, D.R. Nelson, M.J. Coon, R.W. Estabrook, F.J. Gonzalez, F.P. Guengerich, I.C. Gunsalus, E.K. Johnson, B. Kemper B, The P450 superfamily: updated on new sequences, genes mapping, and recommended nomenclature. *DNA Cell Biol.*, 1991, 10, 1-14.

[118] P.A. Williams, J. Cosme, A. Ward, H.C. Angove, D. Matak Vinkovic, H. Jhoti, Crystal structure of human cytochrome P450 2C9 with bound warfarin. *Nature*, 2003, 424, 464-468.

[119] J.K. Yano, M.R. Wester, G.A. Schoch, K.J. Griffin, C.D. Stout, E.F. Johnson, The structure of human microsomal cytochrome P450 3A4 determined by X-ray crystallography to 2.05-A resolution. *J. Biol. Chem.*, 2004, 279, 38091-38094.

[120] M.R. Wester, J.K. Yano, G.A. Schoch, C. Yang, K.J. Griffin, C.D. Stout, E.F. Johnson, The structure of human cytochrome P450 2C9 complexed with flurbiprofen at 2.0-A resolution. *J. Biol. Chem.* 2004, 279, 35630-35637.

[121] P.A. Williams, J. Cosme, D.M. Vinkovic, A. Ward, H.C. Angove, P.J. Day, C. Vonrhein, I.J. Tickle, H. Jhoti, Crystal structures of human cytochrome P450 3A4 bound to metyrapone and progesterone. *Science*, 2004, 305, 683-686.

[122] G.A. Schoch, J.K. Yano, M.R. Wester, K.J Griffin, C.D. Stout, E.F. Johnson, Structure of human microsomal cytochrome P450 2C8. Evidence for a peripheral fatty acid binding site. *J. Biol. Chem.*, 2004, 279, 9497-9503.

[123] J.K. Yano, M.H. Hsu, K.J. Griffin, C.D. Stout, E.F. Johnson, Structures of human microsomal cytochrome P450 2A6 complexed with coumarin and methoxsalen. *Nat. Struct. Mol. Biol.*, 2005, 12, 822-823.

[124] K. Auclair, Z. Hu, D.M. Little, P.R. Ortiz De Montellano, J.T. Groves, Revisiting the mechanism of P450 enzymes with the radical clocks norcarane and spiro[2,5]octane. *J. Am. Chem. Soc.*, 2002, 124, 6020-6027.

[125] A.A. Izzo, Herb-drug interactions: an overview of the clinical evidence. *Fundam. Clin. Pharmacol.*, 2004, 19, 1-16.

[126] C. Gaudineau, R. Beckerman, S. Welbourn, K. Auclair, Inhibition of human P450 enzymes by multiple constituents of the Ginkgo biloba extract. *Biochem. Biophys. Res. Commun.*, 2004, 318, 1072-1078.

[127] J.M. Mathews, A.S. Etheridge, S.R. Black, Inhibition of human cytochrome P450 activities by kava extract and kavalactones. *Drug Metab. Dispos*, 2002, 30, 1153–1157.

[128] L. Zou, M.R. Harkey, G.L. Henderson, Effects of herbal components on cDNA-expressed cytochrome P450 enzyme catalytic activity. *Life Sci.*, 2002, 71, 1579–1589.

[129] L. Zou, G.L. Henderson, M.R. Harkey, Y. Sakai, A. Li, Effects of kava (Kava-kava, Awa, Yagona, *Piper methysticum*) on cDNA-expressed cytochrome P450 enzymes and human cryopreserved hepatocytes. *Phytomedicine*, 2004, 11, 285–294.

[130] D.L. Clouatre, Kava kava: examining new reports of toxicity. *Toxicol. Lett.*, 2004, 150, 85-96.

[131] A.R. Clough, S.P. Jacups, Z. Wang, C.B. Burns, R.S. Bailie, S.J. Cairney, A. Collie, T. Guyula, S.P. McDonald, B.J. Currie, Health effects of kava use in an eastern Arnhem Land aboriginal community. *Int. Med. J.*, 2003, 33, 336-340.

[132] M. Schmidt, A. Nahrstedt, Is kava hepatotoxic? 2002, Online at www.uni-muenster.de/Chemie.pb/Kava/pdf/Review.pdf

[133] Y. Shao, K. He, B. Zheng, Q. Zheng, Reversed-phase high-performance liquid chromatographic method for quantitative analysis of the six major kavalactones in *Piper methysticum*. *J. Chromatogr. A.*, 1998, 825, 1-8.

[134] V.H. Sethy, D.W. Harris, Determination of biological activity of alprazolam, triazolam and their metabolite. *J. Pharm. Pharmacol.*, 1982, 34, 115-116.

[135] L.L. Von Moltke, D.J. Greenblatt, J.S. Harmatz, R.I. Shader, Alprazolam metabolism in-vitro: studies of human, monkey, mouse and rat liver microsomes. *Pharmacology*, 1993, 47, 268-276.

[136] J.C. Almeida, E.W. Grimsley, Coma from the health food store: Interaction between kava and alprazolam. *Ann. Intern. Med.*, 1996, 125, 940-941.

Chapter 3: Conclusion

The aim of the first project was to evaluate the ability of selected molecules to affect the secondary structure of $A\beta_{1-42}$. Molecules stabilizing helical Aβ represent new tools to investigate the role of this conformer in Alzheimer disease. An HPLC method for the purification of crude $A\beta_{1-42}$ was developed and Aβ deaggregation conditions were optimized to ensure consistency and reproducibility of the data. The tested molecules were expected to stabilize the helical $A\beta_{1-42}$ and were designed using three different strategies: 1) analogue of fluorinated solvents; 2) helix-capping, and 3) design based on functional complementarity. The analogue of fluorinated solvents synthesized, bis(2,2,2-trifluoroethyl)malonate, did not affect the secondary structure of $A\beta_{1-42}$ at the concentrations tested. The intermolecular utilization of C- and N-capping molecules, failed to increase helical $A\beta_{(1-42)}$. This suggests that the entropic penalty of binding may have been too high. Finally, the molecules designed based on potential interactions with $A\beta_{1-42}$ side chains, did not succeed in raising the helical content of $A\beta_{1-42}$, suggesting that this strategy requires improvements. Calculation of docking energy for interactions between helical $A\beta_{1-42}$ and the ligands should help better focus our efforts. To this end, collaboration with the laboratories of Dr A. Rank, at the University of Calgary, has recently been established.

The first goal of the second project was to quantify and compare the composition of traditional and commercial kava extracts. The second aim was to compare the effects of these extracts on the activity of human P450 enzymes. Kavalactones were extracted from kava roots using water to mimic the traditional extract, and organic solvents (acetone,

methanol or ethanol) to mimic the different commercial extracts. HPLC quantification of the kavalactones extracted by either of these methods demonstrates that the ratio of kavalactones extracted vary significantly with the nature of the solvent used. Comparison of acetonic, ethanolic and methanolic kava extracts confirms the expected similarity to the commercial caplet extract. The slight variations may be attributed to standardization of the commercial pill extract. *In vitro* experiments with human CYP3A4, CYP1A2, CYP2C9 and CYP2C19 demonstrate that the aqueous, the acetonic and the commercial extracts show different CYP inhibition profiles. When the inhibition of CYP1A2 and CYP2C9 (IC_{50}) are expressed in "μg of extract/ml", the aqueous kava extract shows weaker inhibition compared to the acetonic and the commercial extracts. Results obtained for CYPs 3A4 and 2C19 were similar for the three extracts. On the other hand, when the inhibition (IC_{50}) is expressed in "μg of kavalactone/ml", the values were comparable for all extracts. These results suggest that traditional and commercial kava extracts may cause adverse drug interactions via inhibition of drug metabolism.

At the present time, the reported cases of hepatotoxicity seem to be the result of herb-drug interactions. Two cases were attributed to depletion of CYP2D6. Some studies demonstrate that demethoxyyangonine and dihydromethysticin induce CYP3A2 activity[137]. *In* vivo inhibition studies of CYP1A2 with the traditional kava extract confirm our results[138]. Inhibition of CYPs 1A2, 2C8, 2C9, 2C19, 2D6 and 3A4 by methanolic kava extracts was also confirmed by others[139]. Finally, the few cases of hepatotocixity[140,141,142] reported after kava ingestion without pharmaceuticals are likely idiosyncratic.

Since May 2005, the German government is reconsidering the ban of kava extracts. The re-evaluation of the risk-benefit ratio for kava products will be based on new clinical studies, controlled and conducted at the recommended dosage.

Moreover, the increasing incidence of herb-drug interactions has forced governmental agencies to review their regulations concerning herbal medicines. For example, Health Canada has restructured its Natural Health Product Regulations[143]. The modifications require that importers of natural health products perform quality control investigations at the foreign source sites and submit their report to Health Canada. The owner of the license attributed by Health Canada must ensure that sterile products are manufactured and packaged in separate and closed area under the supervision of microbiologists using validated methods of sterilization. They also need to produce a standard operating procedures for recall of products. Finally, they must provide all clinical study results and adverse events reported for their licensed natural health products. Although it is very far from the requirements for pharmaceuticals, this new regulation is a good initiative to better protect the population.

---

[137] Y. Ma, K. Sachdeva, J. Liu, M. Ford, D. Yang, I.A. Khan, C.O. Chichester, B. Yan, Desmethoxyyangonin and dihydromethysticin are two major pharmacological kavalactones with marked activity on the induction of CYP3A23. *Drug Metab. Dispos.*, 2004, 32, 1317-1324.

[138] S. Russmann, B.H. Lauterburg, Y. Barguil, E. Choblet, P. Cabalion, K. Rentsch, M. Wenk, Traditional aqueous kava extracts inhibit cytochrome P450 1A2 in humans:

Protective effect against environmental carcinogens? *Clin. Pharmacol Ther.*, 2005, 77, 451-454.

[139] M. Unger, A. Frank, Simultaneous determination of the inhibitory potency of herbal extracts on the activity of six major cytochrome P450 enzymes using liquid chromatography/mass spectrometry and automated online extraction. *Rapid Commun. Mass Spectrom.*, 2004, 18, 2273-2281.

[140] R.F.W. Moulds, J. Malani, Kava: herbal panacea or liver poison? *Med. J. Aust.*, 2003, 178, 451–453.

[141] R. Teschke, Kava, kavapyrones and toxic liver injury. *Z. Gastroenterol.*, 2003, 41, 395-404.

[142] J. Anke, I. Ramzan, Kava hepatotoxicity: are we any closer to the truth? *Planta Med.*, 2004, 70, 193–196.

[143] http://www.hc-sc.gc.ca/dhp-mps/prodnatur/legislation/acts-lois/prodnatur/regs_cg2_e.html

ANNEX

Copyright

Quoting "Nixon, Harry (ELS-OXF)" <H.Nixon@elsevier.com>:

We hereby grant you permission to reprint the material mentioned below at no charge in your thesis subject to the following conditions:

1. If any part of the material to be used (for example, figures) has

appeared in our publication with credit or acknowledgement to another source, permission must also be sought from that source. If such permission is not obtained then that material may not be included in your publication/copies.

2. Suitable acknowledgment to the source must be made, either as a footnote or in a reference list at the end of your publication, as follows:

"Reprinted from Publication title, Vol number, Author(s), Title of article, Pages No., Copyright (Year), with permission from Elsevier".

3. Reproduction of this material is confined to the purpose for which permission is hereby given.

4. This permission is granted for non-exclusive world English rights only. For other languages please reapply separately for each one required. Permission excludes use in an electronic form. Should you have a specific electronic project in mind please reapply for permission.

5. This includes permission for the National Library of Canada to supply single copies, on demand, of the complete thesis. Should your thesis be published commercially, please reapply for permission.

Yours sincerely

Harry Nixon

Rights Assistant
Global Rights Department
Phone - 0044 (0) 1865 843517
Fax - 0044 (0) 1865 853333

Email - H.Nixon@Elsevier.com